

**CASE FILE**  
**COPY**

**NASA**

**MEMORANDUM**

1958 NASA/USAF SPACE PROBES

(ABLE-1)

FINAL REPORT

VOLUME 1. SUMMARY

By Space Technology Laboratories, Inc.  
Los Angeles 45, Calif.

**NATIONAL AERONAUTICS AND  
SPACE ADMINISTRATION**

WASHINGTON

June 1959

NASA MEMO 5-25-59W VOL. 1



## 1.1 Introduction

Early in calendar year 1958 Space Technology Laboratories, Inc. (STL) (then Space Technology Laboratories, a division of the Ramo-Wooldridge Corp.) developed for the Air Force Ballistic Missile Division (AFBMD) an Advanced Re-entry Test Vehicle (ARTV) for the purpose of testing ballistic missile nose cones at the full range of 5500 nautical miles. The two-stage ARTV utilized the Thor ballistic missile and the second stage propulsion system developed for the Vanguard program.

In late 1957 and early 1958, STL/AFBMD prepared studies of various missile combinations which could be utilized for space testing. The Thor, in combination with the Vanguard second and third stages, was one of the vehicles considered which offered a very early capability of placing a reasonable payload in a lunar orbit. These STL/AFBMD studies were presented to various appropriate groups including the Killian, Millikan, H. J. Stewart Committees; Headquarters, Air Research and Development Command, and ARDC Centers.

Subsequently the Advanced Research Projects Agency (ARPA) contacted STL relative to the availability of hardware for an early lunar shot. By utilizing existing spares already purchased for the ARTV, and by making use of the ARTV contractors already in being, it appeared feasible to launch by the third quarter of calendar year 1958 a payload which would be captured by the moon's gravitational force.

On 27 March 1958, ARPA directed STL to proceed with a program of three lunar shots. As much as possible, these shots were to utilize existing ARTV spare hardware and impose no interference with the ballistic missile programs. In September this program was transferred to the direction of the National Aeronautics and Space Administration (NASA).

On 17 August 1958 the first launching of the Able-1 vehicle was attempted, but the flight was terminated by a propulsion failure of the first stage. Subsequent launchings were attempted on 13 October and 8 November 1958. Of these launchings the October attempt was the most successful. Although the payload did not reach the vicinity of the moon, a maximum altitude of 71,700

miles was attained, and useful scientific data was obtained from the instrumentation. Although the maximum altitude attained during the November launching was only 970 miles, useful scientific data was also obtained in this flight. Failure of the third stage to ignite limited the maximum altitude reached on this flight.

The primary objectives of the program were successfully met by the October shot, which were to obtain scientific data in cislunar space.

In the interval between program approval and the first launch the following new subsystems were completely developed and tested: payload, including payload structure, the scientific instrumentation, payload telemetry, a command/doppler system, and vernier velocity correction system. The ARTV vehicle was modified to accept the third stage and payload. A ground tracking network was established, including STL stations at Hawaii, Jodrell Bank (near Manchester, England), Singapore, and these stations were designed, constructed, and tested in the same time interval

Figure 1-1 shows the Able-1 four-stage vehicle on stand at AFMTC. The nominal trajectory for the three flights is shown in Figure 1-2(a), while Figure 1-2(b) plots the actual trajectory for Flight 2.

## NASA MEMO 5-25-59W

## Note

The record of the 1958 NASA/USAF Space Probes is presented in four volumes. This summary (Volume 1) will meet the needs of most readers. The other three volumes present details that are of value to specialists. Volume 2 deals with the payload and experiments; Volume 3 with the vehicles, trajectories, and flight histories; and Volume 4, which is classified confidential, with the characteristics of the engines.

Qualified requesters may obtain copies of the several volumes from the

Technical Information Division  
Code BID  
National Aeronautics and Space Administration  
Washington 25, D. C.



1958 NASA/USAF SPACE PROBES

(ABLE-1)

FINAL REPORT

VOLUME 1. SUMMARY

Prepared for Air Force Ballistic Missile Division  
Headquarters A R D C  
Under Contract AF 04(647)-205

18 February 1959

SPACE TECHNOLOGY LABORATORIES, INC.  
P. O. Box 95001  
Los Angeles 45, California





# CONTENTS

	Page
1.1 Introduction . . . . .	1
1.2 Payload . . . . .	5
1.2.1 Payload Vehicle Characteristics . . . . .	5
1.2.1.1 Payload Configuration . . . . .	5
1.2.1.2 Antennas . . . . .	7
1.2.1.3 Power Supply . . . . .	9
1.2.2 Experiments . . . . .	11
1.2.2.1 Ion Chamber Experiment . . . . .	11
1.2.2.2 Proportional Counter Telescope . . . . .	14
1.2.2.3 Conclusions and Inferences Which may be Drawn from Pioneer I and Pioneer II Cosmic Ray Experiments . . . . .	20
1.2.2.4 Magnetometer . . . . .	25
1.2.2.5 Micrometeorite Detector . . . . .	30
1.2.2.6 Temperature Measurement . . . . .	37
1.2.2.7 STL Television . . . . .	40
1.2.3 Telemetry . . . . .	44
1.2.3.1 Transmitters . . . . .	44
1.2.3.2 Subcarrier Oscillators . . . . .	44
1.2.3.3 Data Collection for Flight 2 . . . . .	45
1.2.3.4 Data Collection for Flight 3 . . . . .	47
1.2.4 Command/Doppler System . . . . .	48
1.2.4.1 General . . . . .	48
1.2.4.2 System Characteristics . . . . .	49

CONTENTS (Continued)

	Page
1.2.4.3 Final Performance Characteristics . . . . .	55
1.3 Vehicle Characteristics . . . . .	57
1.3.1 Trajectory Considerations . . . . .	57
1.3.2 Design Characteristics . . . . .	57
1.3.3 Evaluation of Design . . . . .	61
1.4 Tracking and Communications . . . . .	64
1.4.1 Ground Stations . . . . .	64
1.4.1.1 Description of Ground Station Subsystems . . . . .	64
1.4.1.2 Tracking Techniques . . . . .	65
1.4.1.3 Data Reduction and Storage . . . . .	66
1.4.1.4 Ground Station Communications and Data Transmission . . . . .	66
1.4.1.5 Special Tracking and Photographing Task with an Astronomical Telescope . . . . .	66
1.4.1.6 Communications Office, AFMTC . . . . .	69
1.4.1.7 Hawaii . . . . .	69
1.4.1.8 Manchester . . . . .	71
1.4.1.9 Singapore . . . . .	73
1.4.1.10 Millstone . . . . .	73
1.4.1.11 Malabar Station, Melbourne, Florida . . . . .	73
1.4.1.12 Army Ballistic Missile Agency . . . . .	74
1.4.2 Functioning of Ground Stations During Flights . . . . .	74
1.4.2.1 AFMTC Station . . . . .	74
1.4.2.2 Millstone Station . . . . .	74
1.4.2.3 Manchester Station . . . . .	74

CONTENTS (Continued)

	Page
1.4.2.4 Hawaii Station . . . . .	74
1.4.2.5 Singapore Station . . . . .	75
1.4.3 Data Handling: Able-1 Operations Center . . . . .	75
1.4.4 Trajectory Determination for Specific Flights . . . . .	76
1.4.4.1 August Flight - Missile 127 . . . . .	76
1.4.4.2 October Flight - Missile 130 . . . . .	76
1.4.4.3 November Flight - Missile 129 . . . . .	77
1.5 Flight Summaries . . . . .	82
1.5.1 First Lunar Probe . . . . .	82
1.5.2 Second Lunar Probe . . . . .	82
1.5.3 Third Lunar Probe . . . . .	84



## ILLUSTRATIONS

Figure		Page
1- 1	Able-1 Vehicle . . . . .	3
1- 2(a)	Powered Flight Profile . . . . .	4
1- 2(b)	Pioneer I, Projection of the Vehicle in the Plane of the Moon's Orbit. . . . .	4
1- 3	Pioneer Payload Package . . . . .	6
1- 4	Two Paint Patterns for Temperature Control . . .	8
1- 5	Payload Showing Antennas. . . . .	10
1- 6	Ionization Chamber . . . . .	13
1- 7	Pioneer I Ionizing Radiation Versus Distance from the Surface of the Earth . . . . .	15
1- 8	Pioneer II Ionizing Radiation Versus Distance from the Surface of the Earth Including Longitudes and North Latitudes . . . . .	16
1- 9	Ionization Versus Latitude at an Altitude of $\pm 25$ km	17
1-10	Proportional Counter Telescope . . . . .	19
1-11	University of Chicago Proportional Counter Telescope Triples Rate . . . . .	21
1-12	Magnetometer . . . . .	26
1-13	$B_{\perp}$ Component of Magnetic Field in $\Gamma$ vs. Distance from Center of Earth (Pioneer I). . . . .	28
1-14	AFCRC Micrometeorite Detection System . . . . .	31
1-15	Micrometeorite Experimental Apparatus. . . . .	32
1-16	Micrometeorite Collisions Recorded by Low Momentum Experiment . . . . .	34
1-17	Micrometeorite Collision Recorded by High Momentum Experiment . . . . .	35
1-18	Temperature Versus Radial Distance from Earth's Surface for Pioneer 1 . . . . .	38

ILLUSTRATIONS (Continued)

Figure		Page
1-19	Temperature History of Pioneer II . . . . .	39
1-20	Illustration of TV System Operation . . . . .	41
1-21	Sampling Scheme Shown for Two Spin Cycles . . . . .	43
1-22	Telemetry Reception at Various Stations (Flight 2) . . . . .	46
1-23	Simplified Block Diagram, Doppler Transponder and Command Receiver . . . . .	50
1-24	Doppler and Command Receiver . . . . .	51
1-25	Basic Airborne Phase-Locked Loop and Transponder . . . . .	53
1-26	Ground Communication Net . . . . .	67
1-27	Ground Station Network . . . . .	68
1-28	The Hawaii Ground Station . . . . .	70
1-29	Manchester Tracking Station Showing STL Facility . . . . .	72
1-30	Actual Tracking Data of Manchester Compared with Theoretical Tracking . . . . .	78
1-31	Projection on Earth of Path of Flight 2 . . . . .	79
1-32	Pioneer II, Projection of the Path of Flight 3 on the Earth's Surface . . . . .	81

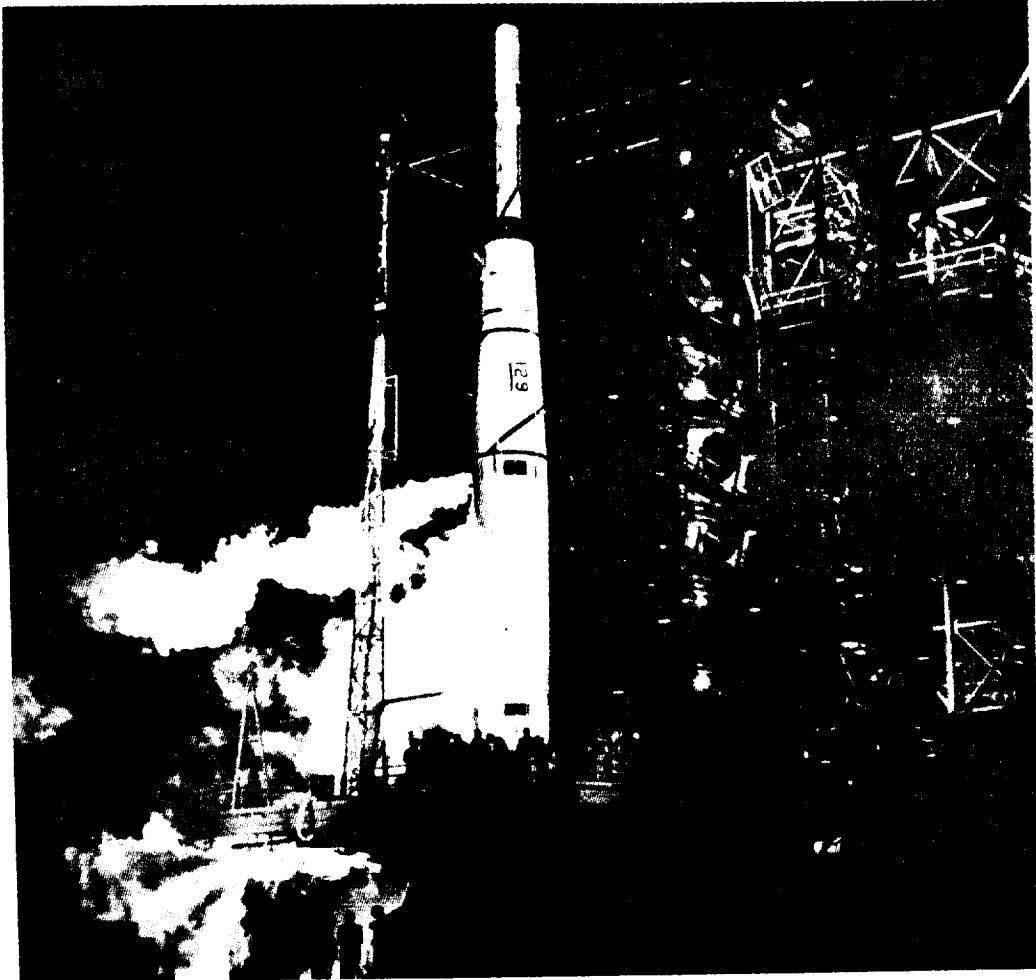


Figure 1-1. Able-1 Vehicle.

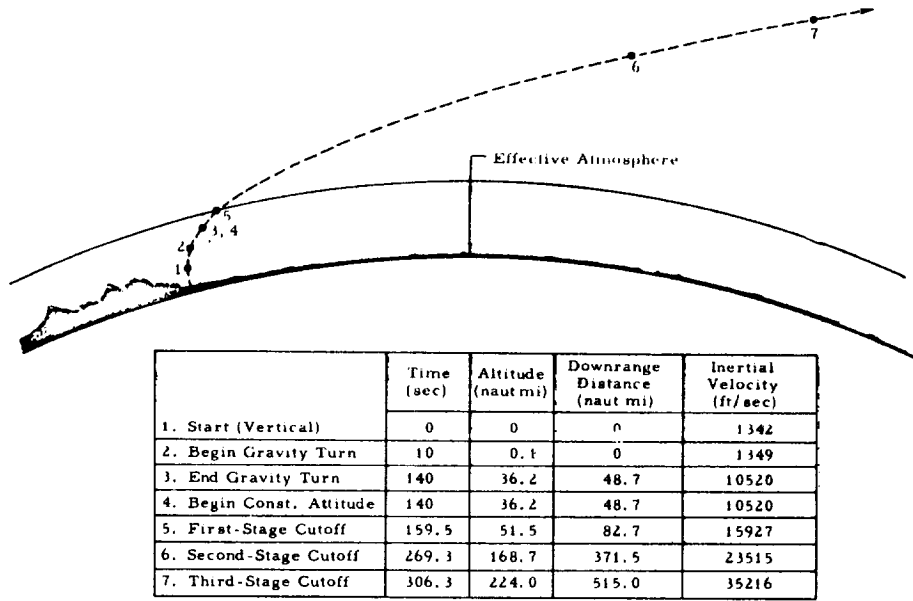


Figure 1-2(a). Powered Flight Profile.

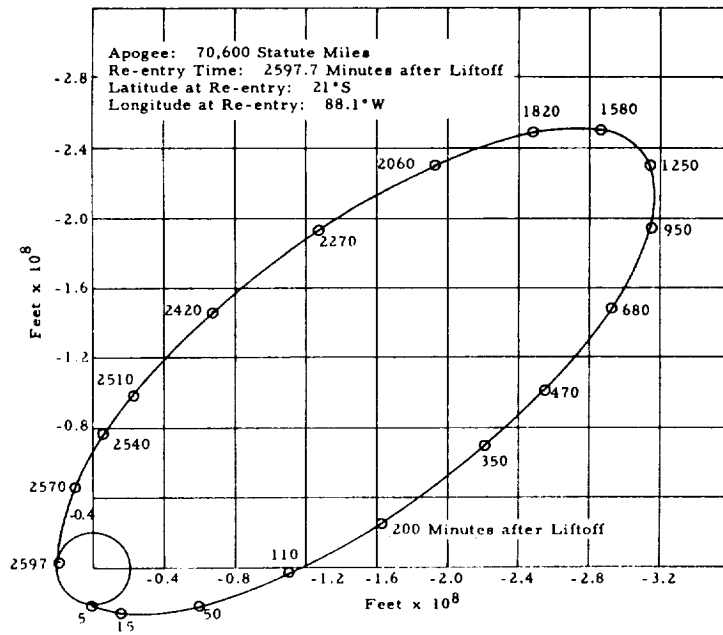


Figure 1-2(b). Pioneer I, Projection of the Vehicle in the Plane of the Moon's Orbit.



## 1.2 Payload

### 1.2.1 Payload Vehicle Characteristics

The final payload was designed so that, within the stringent weight limits, the greatest amount of data could be gathered from the widest variety of experiments, and so its electrical system would have the maximum possible life. Subminiaturization and multi-power devices would have to be employed to the greatest extent possible without impairing circuit power, efficiency, or reliability. Other considerations that influenced the design were (1) the ambient thermal properties of the vehicle, (2) dynamic stability, (3) experimental environment, and (4) the necessity to make quick prelaunch emergency repairs and calibration checks.

#### 1.2.1.1 Payload Configuration

The payload was designed to carry appropriately mounted experimental instrumentation and to meet the particular requirements of the mission. The vehicle had to be dynamically stable to maintain the correct orientation of the retrorocket as well as the correct orientation of the experimental instrumentation. In addition, it was necessary that the payload package be nonconducting to meet antenna requirements. Moreover, the payload had to be designed in such a way as to maintain the temperature within the vehicle within a specified range. Figure 1-3 is a photograph of the Pioneer I payload.

##### (a) Dynamic Stability

Three steps taken to ensure dynamic stability of the vehicle in inertial space were: (1) the payload weight was distributed in a manner which provided suitable moments of inertia; (2) a spin of approximately two revolutions per second was imparted to the payload; and (3) a damper ring was used to damp out precessional motions.

##### (b) Temperature Control

Temperature control of the payload was effected by proper selection of the ratio of solar absorptivity to long wave length emissivity of the surface material. Since the payload was nonspherical, the projected area intercepting solar energy varied with the sun look-angle. The curve of projected area as a function of sun look-angle was nonlinear so that at certain sun angles the amount of solar energy intercepted and consequently the payload mean temperature was quite sensitive to changes in attitude angle. At other

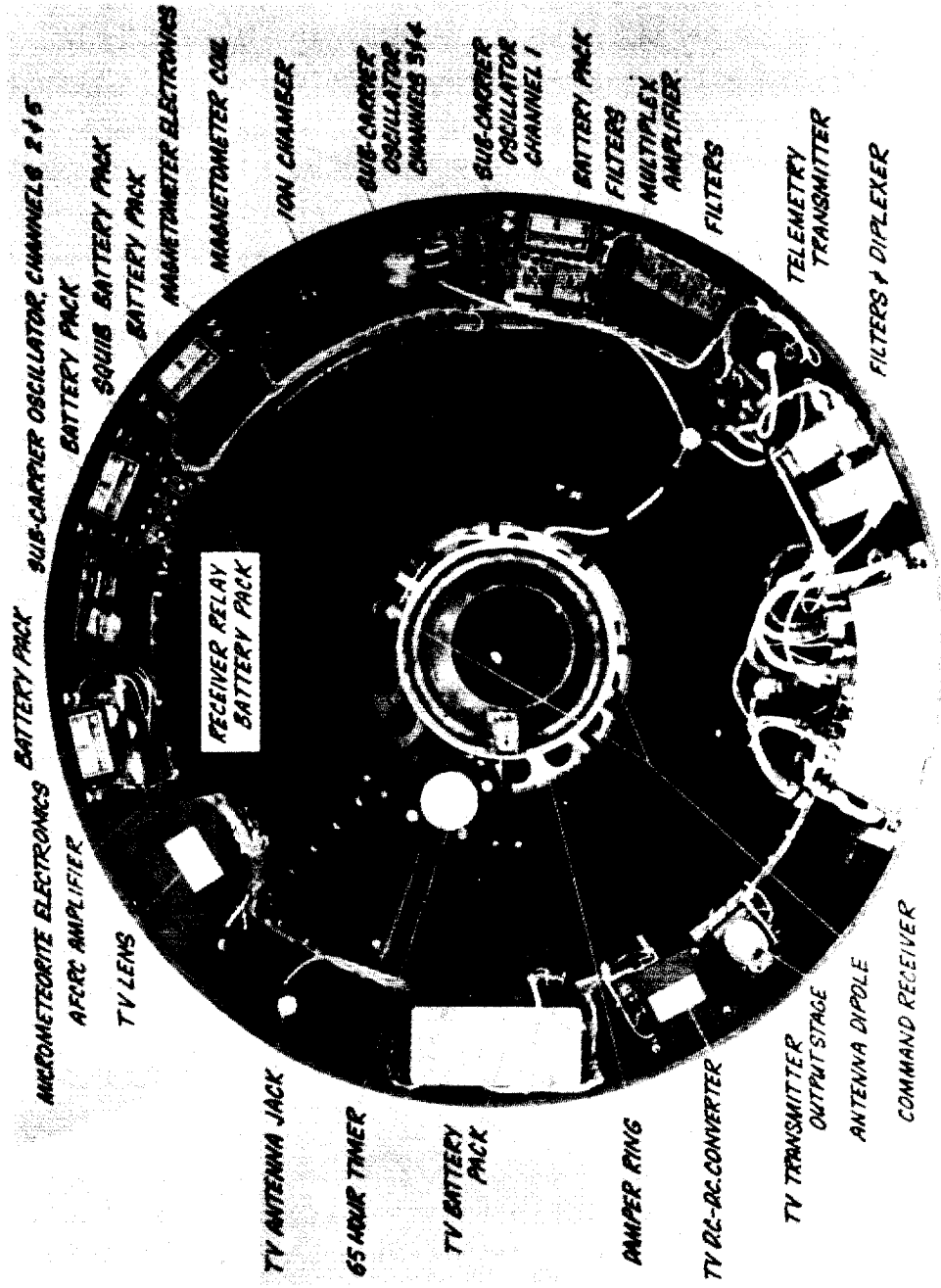


Figure 1-3. Pioneer Payload Package.

sun look-angles the intercepted area was relatively insensitive to changes in angle. Because of the rotation of the earth-moon system around the sun, the look-angle changed about one degree per day during flight or about 10 degrees for the expected useful life of the flight. This resulted in temperature changes well within allowable limits even at the most sensitive region of the curves of intercepted area as a function of sun look-angle.

Operational requirements made it quite possible that the payload prepared for a given launch date would have to be readied within a relatively few hours for the next launch date. Such rapid changes of absorptivity-to-emissivity ratio were achieved by the addition or removal of paint tapes of the proper area, to yield the desired mean value of the ratio for the new launch date. Figure 1-4 shows two paint patterns.

(c) Structure

Because the magnetometer experiment was intended to measure the magnetic fields existing in space around the payload, any magnetic materials or magnetized objects which might distort the observed field were highly undesirable. It was therefore necessary to keep the mass of such materials to an irreducible minimum, and to place the magnetometer coil as far as possible from those magnetic materials which must be included in the payload.

In addition, to comply with antenna requirements it was necessary to introduce a series of radial conductors in order to provide a ground plane for the antennas.

The payload structure was therefore made of a hexcel core of nylon and phenolic glass cloth bonded to epoxy-impregnated glass cloth sheets. It consists of a cylinder 29 inches in diameter and 6 inches long, with cone frustums approximately 6-1/2 inches high. The aft frustum has a local reinforcement shelf for the support of the payload experiments. Metal fittings are inserted in appropriate locations for support loading and for attachment to adjoining structures.

1.2.1.2 Antennas

The antenna system for Pioneer I included both an electric and a magnetic dipole. The magnetic dipole was used for the NOTS television

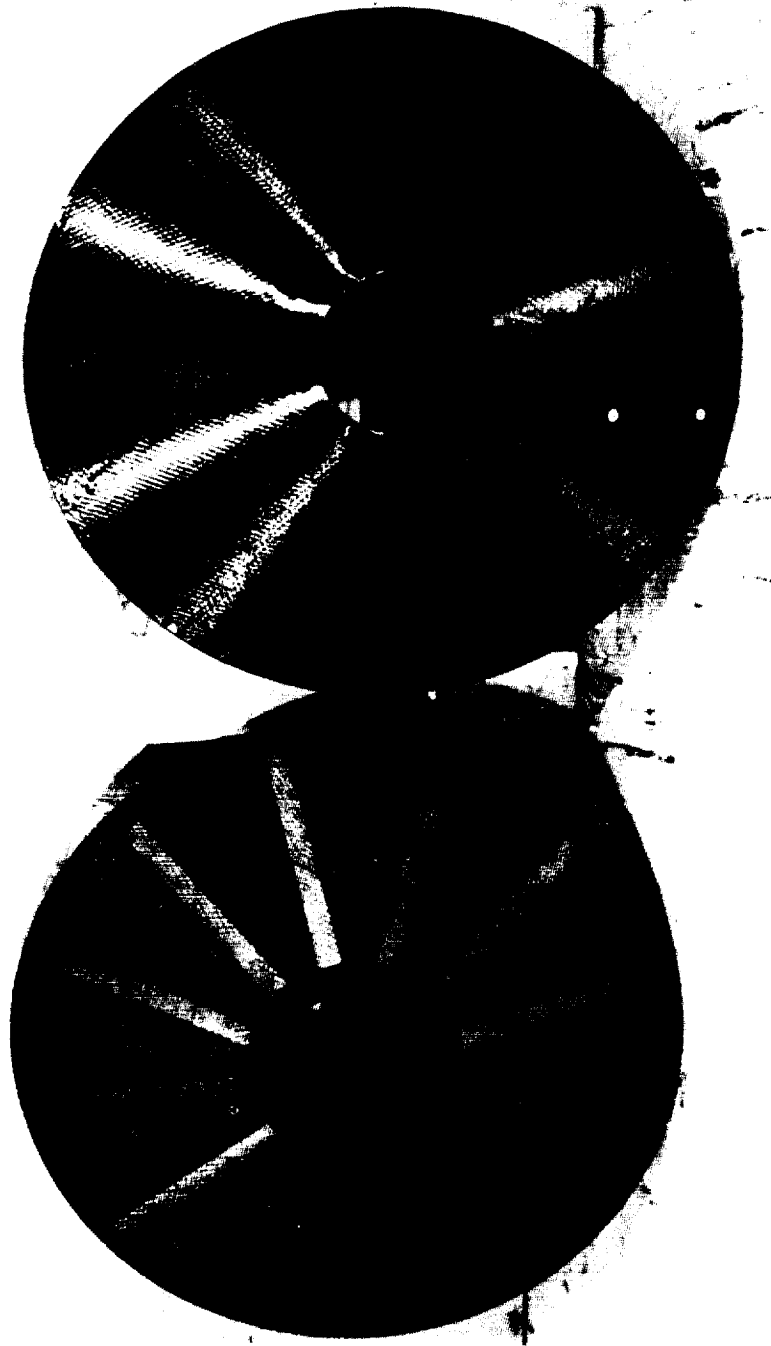


Figure 1-4. Two Paint Patterns for Temperature Control.

system which operated on 108.09 mc at a peak power of 50 watts. The electric dipole was used for the 108.06 mc STL telemetry transmitter. The pattern of this dipole was adjusted to be as closely omnidirectional as possible. On Pioneer II, both antennas were left in place, the magnetic dipole being utilized for the 108.09-mc transmitter and the electric dipole antenna being utilized for the 108.06-mc transmitter as on Pioneer I.

The antenna systems for the payload as developed by the STL Antenna Laboratory were capable of transmitting signals to the tracking stations at 108.06 mc and at 108.09 mc and also of receiving command signals at 114.813 mc. Figure 1-5 shows the payload antennas. The electric dipole system was used not only to transmit the 108.06-mc signal but because of its broader band to receive the 114.813-mc command signal.

#### 1.2.1.3 Power Supply

In the Able-1 payload, three different d-c power supplies were used. Mercury batteries were selected because of their favorable shelf life, watt hours per pound ratio, and their ability to work in a vacuum. The NOTS TV used the Yardney silver cell type battery, which gives higher delivery rates of current for short periods of time. The Goulton nickel-cadmium storage battery was selected by STL for the rocket ignition circuit because of its ability to deliver current in a hermetically sealed container and still remain under a specified weight allowance.

It was also decided that each electrical component should carry its own power supply so that the failure of one power supply would not jeopardize the operation of other electrical equipment. Approximately 16 separate power packs were used to supply power to such equipment as the command receiver, ion chamber, cosmic ray telescope, etc.

Except for the mercury batteries that failed to close the command circuit relays on the payload of Flight 2 because the cold reduced their output, the power supply on all the lunar probes operated satisfactorily and verified design specifications. The electrical output of the mercury batteries was almost doubled on Flight 3 in order to insure current capability under adverse environmental conditions such as those experienced in Flight 2.

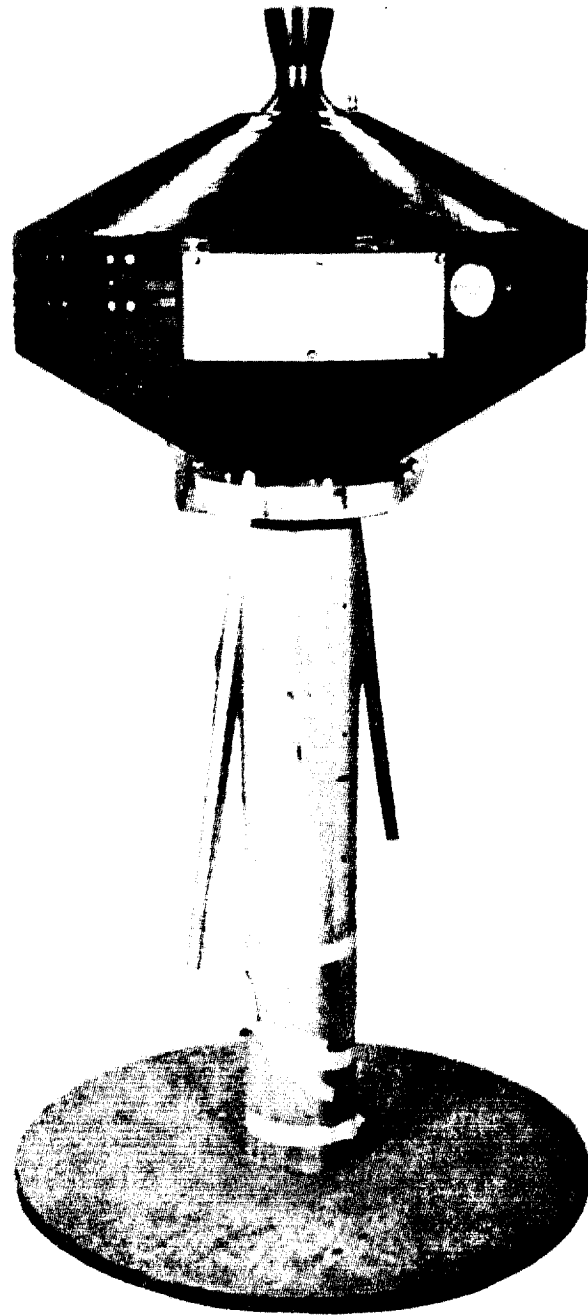


Figure 1-5. Payload Showing Antennas.

### 1.2.2 Experiments

To the maximum extent possible, within the weight and power restrictions, experiments were designed to obtain scientific measurements of the environment in cislunar space. A magnetometer experiment was devised to measure the earth's and the moon's magnetic fields. The flux and approximate energy spectrum of micrometeorites was measured. Two facsimile television systems, a Naval Ordnance Test Station design on the first flights and an STL system on the last, were included. Internal payload temperature was measured. To measure radiation in space, an ion chamber was installed in Flight 2. For Flight 3 this experiment was augmented by a University of Chicago proportional counter.

#### 1.2.2.1 Ion Chamber Experiment

An ion chamber measures the number of ion pairs produced in the volume of the chamber. It was first used for the purpose of determining the flux of X-rays or gamma radiation in the air.

In order to analyze the results of experiments performed with ionization chambers, it is necessary to consider the response of the chamber to a wide variety of particles and energies. Besides the response to primary cosmic rays, the chamber will respond to secondary mesons, protons, beta particles, and gamma rays. These secondaries result from interaction of the primary particles with the walls of the chamber and with the material surrounding the ion chamber. High-energy primary radiation may cause shower cascades (spallation reactions or stars) so that the number of secondaries produced by a single primary may be as high as 50 penetrating particles. The ionization due to such a shower may be increased by a factor of 50, when compared to the ionization due to the original primary.

It thus becomes clear that the ion chamber can at most yield a qualitative idea of the nature of the radiation present in outer space. Probably only a versatile spectrometer could give a quantitative measure of the kinds and their energy distributions. However, problems of weight, power, complexity, and, in particular, problems relating to the environment of space

prohibited the use of such a device on the Able-1 flights. Therefore, the ion chamber is most suitable to determine the biological damage which a living organism might undergo if it were situated in the payload. The ion chamber thus yields a direct measure of the number of REM\* in the region where the chamber is located. The total energy loss of radiation within a given volume is the closest one can come to measuring the biological effect of penetrating radiation with a nonbiological experiment.

#### 1.2.2.1.1 Description

The ionization chamber, which was designed by J. A. Van Allen, State University of Iowa, consisted of an aluminum-walled vessel filled with spectroscopically pure argon to a pressure of 200 lb/in.<sup>2</sup> at 20°C. Volume of the chamber was 43 cm<sup>3</sup> and the areal density of the walls was 400 mg/cm<sup>2</sup>. The electronics followed a design utilized for the CsI scintillation count-rate meter in the Explorer IV.\*\* A d-c electrometer amplifier, with a range of 10<sup>7</sup> roentgens per hour, drove a subcarrier oscillator which, in turn, modulated the transmitter. In-flight calibration utilized a stable multivibrator which substituted a known potential in place of the ionization chamber output. This substitution occurred for a 20-second period once each 200 seconds. Figure 1-6 is a photograph of the entire experimental equipment.

Empirical calibration of the chamber was accomplished utilizing a Co<sup>60</sup> bomb at the Radiology Department of the UCLA Medical Center. A post-flight comparison of these data with the estimated sensitivity disclosed a discrepancy which was interpreted to mean the the ion chamber had leaked.

---

\* REM is defined as the amount of ionizing radiation which when absorbed by living tissue produces an effect equivalent to 1 roentgen of gamma radiation at 400 KEV

\*\* J. A. Van Allen, C. E. McIlwain, and G. H. Ludwig, "Radiation Observations with Satellite 1958 Epsilon" (preprint of an article to be published in the Journal of Geophysical Research).



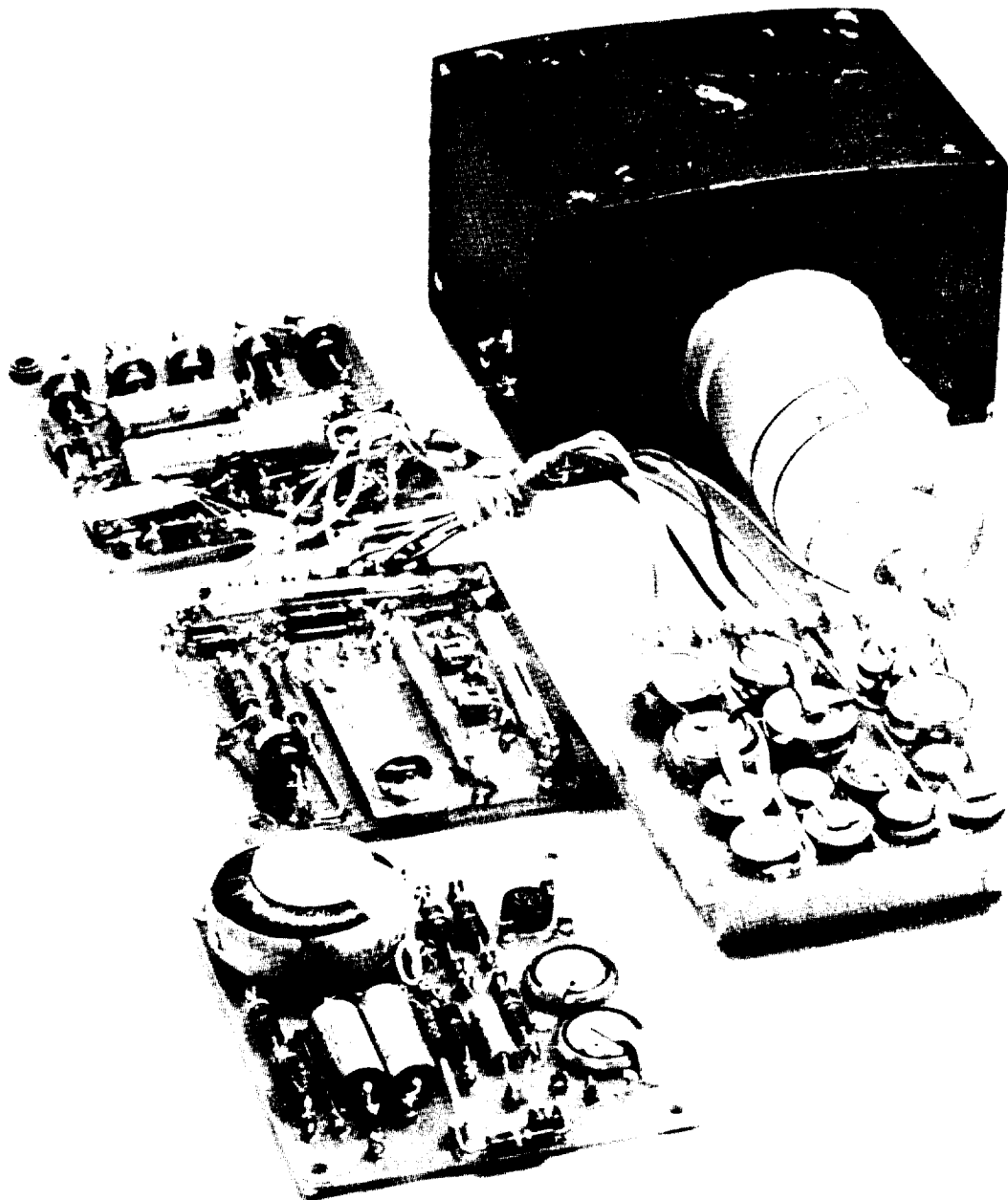


Figure 1-6. Ionization Chamber. Shown above is the ion chamber and associated electronic circuitry. In the upper right-hand corner is the in-flight calibration multivibrator. Just below, is the electronic amplifier; at the bottom of the photo is the subcarrier oscillator and to the left is the battery pack.

The empirical calibration indicates that 1 roentgen per hour corresponds to  $(1.6 \pm 0.05) \times 10^{-11}$  ampere. Estimated sensitivity, determined from the mass of argon and the energy formation of an ion pair, is  $8.9 \times 10^{-11}$  ampere per roentgen per hour.

The apparatus used in Pioneer II was essentially the same as that used in Pioneer I. The major changes were a reduction of the temperature sensitivity of the circuits by a careful choice of circuit components, and a reduction in the range of values of ionization to which the circuit was sensitive. Ion chamber data were received during the first half hour of flight.

#### 1.2.2.1.2 Results

Figures 1-7 and 1-8 plot the ionizing radiation measured in roentgens per hour versus altitude for Flight 2 (Pioneer I) and Flight 3 (Pioneer II). Since the doppler command transmitter was on, no telemetry was received until 2000 nautical miles on Flight 2. However, a radiation belt is clearly indicated between 2000 and 13,000 nautical miles. At 6000 nautical miles, where a maximum of 10 roentgens per hour was found, an average man would receive a lethal dose in about 50 hours. Although the measurements were different, the extrapolated curve is in good agreement with the later Pioneer III flight data.

The information on ionizing radiation gathered during the brief life of Pioneer II clearly indicates an increase of such radiation with decreasing north latitudes. At the apogee of the orbit, in the altitude range of 1470 to 1520 km, the vehicle traversed  $7^\circ$  of latitude from  $30^\circ\text{N}$  to  $23^\circ\text{N}$  latitude. Thus, for essentially constant altitude, a variation of ionization with latitude was observed. Figure 1-9 shows the variation of ionization with latitude when the chamber was located in the 50-km range between 1470 to 1520-km altitude. Since these data show the radiation increasing greatly near the geomagnetic equator, it appears that the trapping of the particles follows a pattern similar to the earth's measured geomagnetic field.

#### 1.2.2.2 Proportional Counter Telescope

In order to determine whether or not a heliocentric and geocentric disordered magnetic field is energy dependent to incoming cosmic radiation,

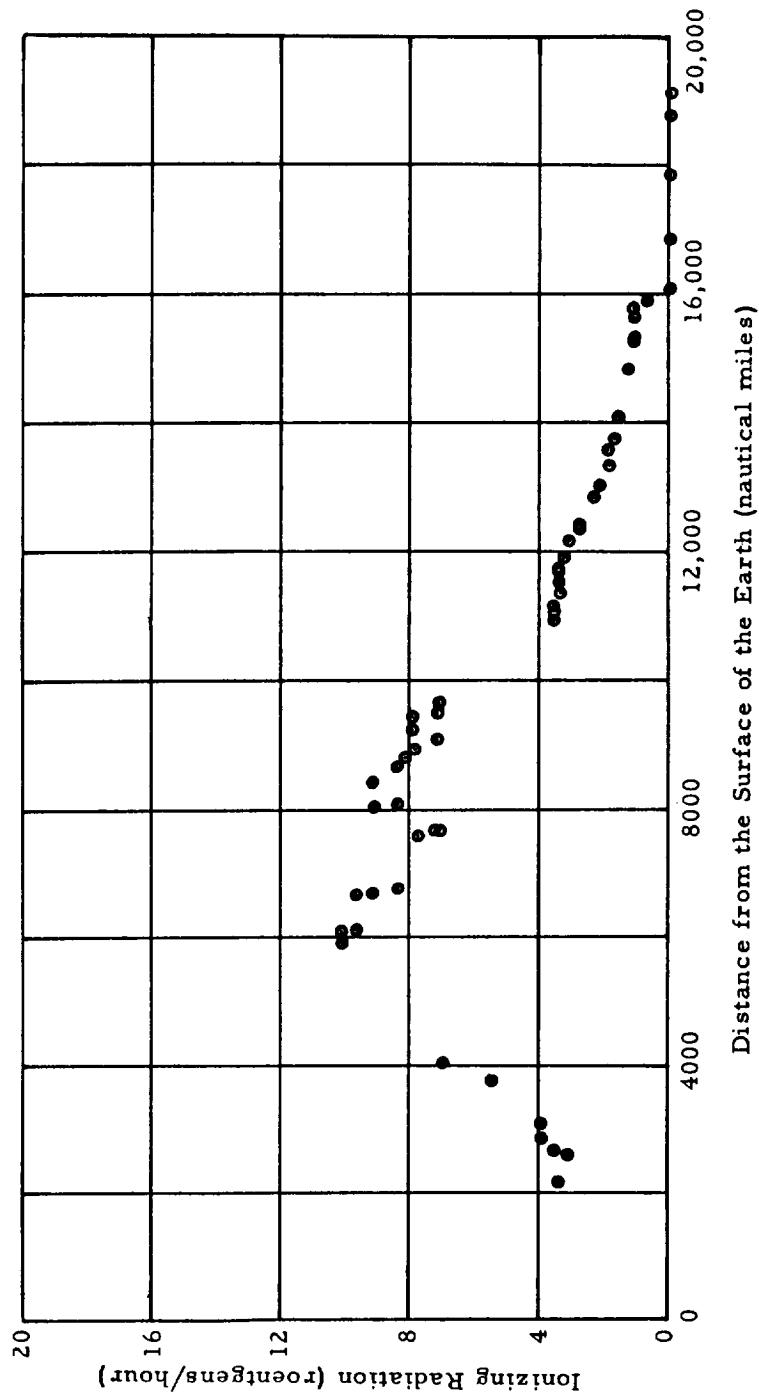
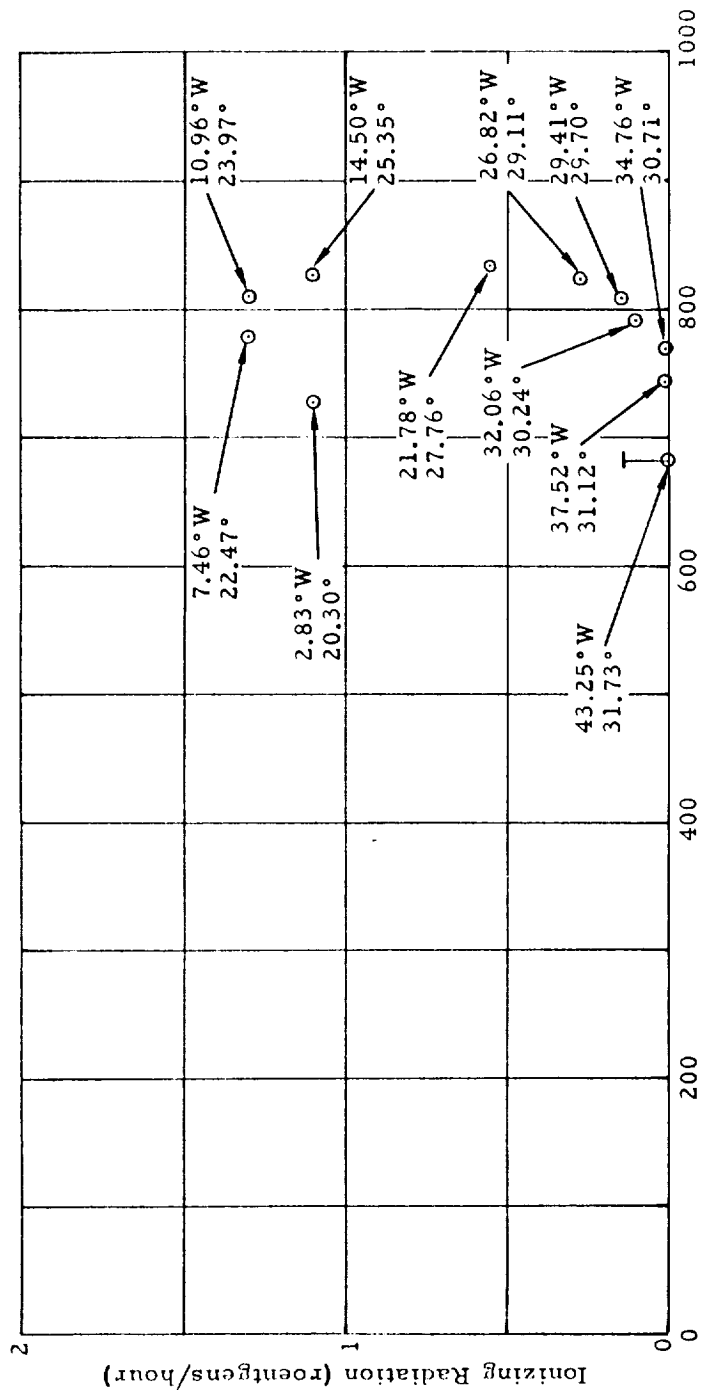


Figure 1-7. Pioneer I Ionizing Radiation Versus Distance from the Surface of the Earth.



Distance from the Surface of the Earth (nautical miles)

Figure 1-8. Pioneer II Ionizing Radiation Versus Distance from the Surface of the Earth Including Longitudes and North Latitudes.

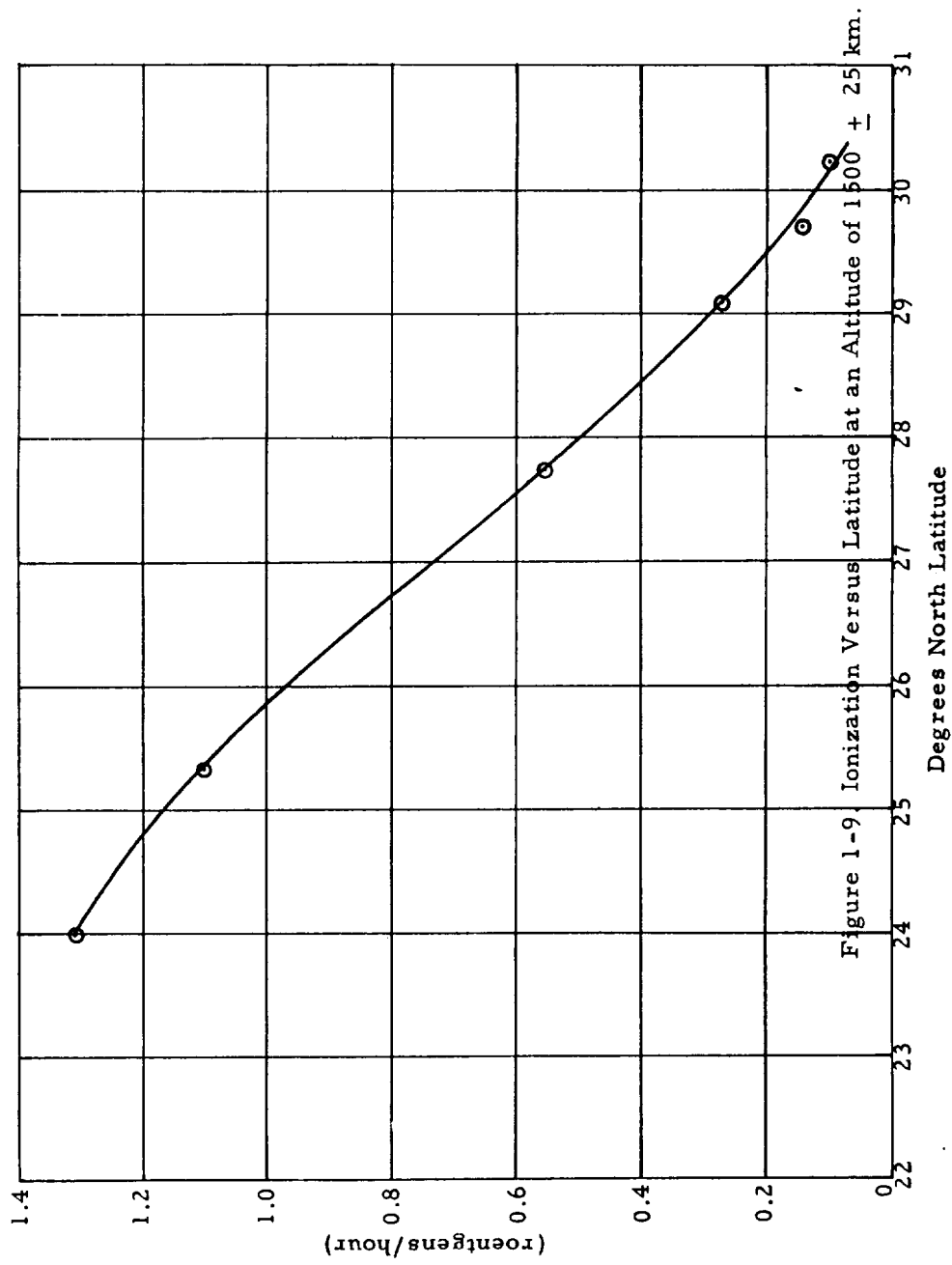


Figure 1-9. Ionization Versus Latitude at an Altitude of 1500 ± 25 km.

the University of Chicago proposed to ARPA that a proportional counter telescope be carried on the Able-1 flights. At the direction of ARPA this experiment was constructed for inclusion in the third flight (Pioneer II).

#### 1.2.2.2.1 Description

The proportional counter had a 1-cm tube, 2 inches in length, surrounded by six others of the same size in a concentric arrangement about the center tube. The counters were filled to 60-cm pressure with a mixture of 40 per cent methane and 60 per cent argon, yielding with associated amplifiers a resolving time of 1 microsecond. The center wires were 1 mil tungsten and the counter was 1 gm/cm<sup>2</sup> brass. The whole assembly was contained in a lead shield of thickness 5 gm/cm<sup>2</sup> (Figure 1-10). In addition to the single events counted by the center tube, triple events occurring in the center tube and any two others diametrically opposed were counted by having the three outputs connected to a triple coincidence circuit which was in turn connected to a scaler chain.

The counters are gamma sensitive although the low photoelectric conversion efficiency in the counter walls tends to reduce the sensitivity and the triple coincidence channel has a relatively narrow solid angle for a coincidence (though the acceptance solid angle is almost  $4\pi$  steradians). Thus, the gamma coincidence rate will be further reduced because of the high scattering cross section for gammas. The shielding corresponds to the stoppage of a 50-Mev electron in the case of nominal incidence.

It was planned to observe the single rates and triple coincidence rates as a function of radial distance from the earth, and thus to obtain data on whether the existing minimum on the earth (due to the present solar activity maximum) changes and whether the counting rate increases and approaches a plateau characteristic of the cosmic ray level during inactive solar years. If during the cislunar flight such an increase were observed, the disordered field mechanism would then be scaled in size.

The equipment was intended to be kept as isotropic in response as possible, the singles and triples events allowing some separation in range.

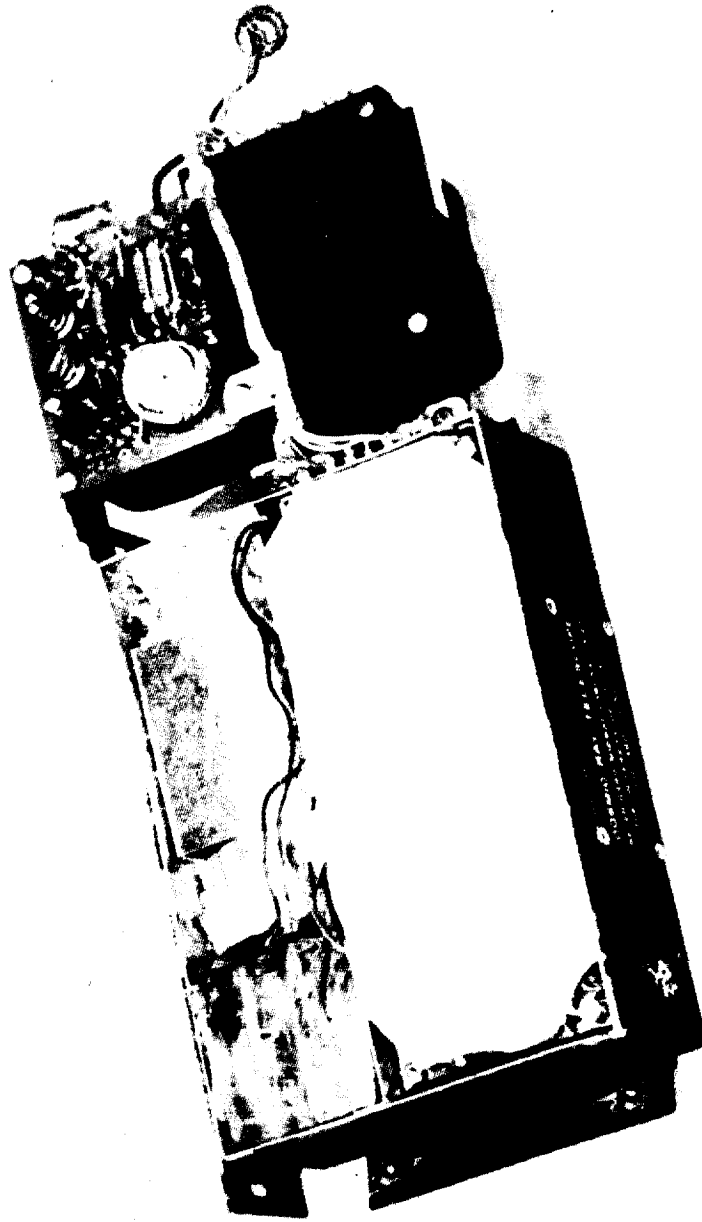


Figure 1-10. Proportional Counter Telescope.

The triple coincidence circuit was introduced some time after the initial design had begun its additional purpose, to serve as an adjunct to the ion chamber experiment and thus help map the radial distribution in the high flux about the earth. By utilizing such a triple channel, the expected counting rate could be held to a tolerable level and not block the scalers.

#### 1.2.2.2.2 Results

Figure 1-11 shows the observed triples rate as a function of altitude. As the vehicle approached the equator the triples counting rate became so high that the telemetry could no longer respond. No data was obtained from the singles channel predominantly because the telemetry apparently did not lock on this frequency. However, it is possible, for example, that the count rate was so high that it was not possible for the telemetry to lock on a single frequency.

#### 1.2.2.3 Conclusions and Inferences Which May Be Drawn From Pioneer I and Pioneer II Cosmic Ray Experiments

Conclusions may be drawn from the direct observations apparent from the reduced data. Much of this has already been presented in graphic form. On the other hand, inferences may be drawn from comparing the ion chamber data with the proportional counter data and from correlating these observations with the observations of the Explorer series of satellites. It is possible to make some useful observations relative to the series of particles present in the radiation belts and their energies. Inferences concerning the geomagnetic field as well as the trapping mechanism are also possible. Moreover, it is expected that the average specific ionization of the particles will be accurately determined when the proportional counter experiment has been sufficiently analyzed.

##### 1.2.2.3.1 Direct Observation

The first type of conclusion that can be drawn from the data consists of direct observations. These can be outlined briefly as follows:

- a. The first experimental verification of the existence of a confined radiation zone of the type postulated by Van Allen et al<sup>\*</sup> was made.

<sup>\*</sup>Van Allen, J. A., Ludwig, G. H., Ray, E. C., and McIlwain, C. E., IGY Satellite Report Series, Number 3, National Academy of Sciences, National Research Council, Washington 25, D. C., 1 May 1958.



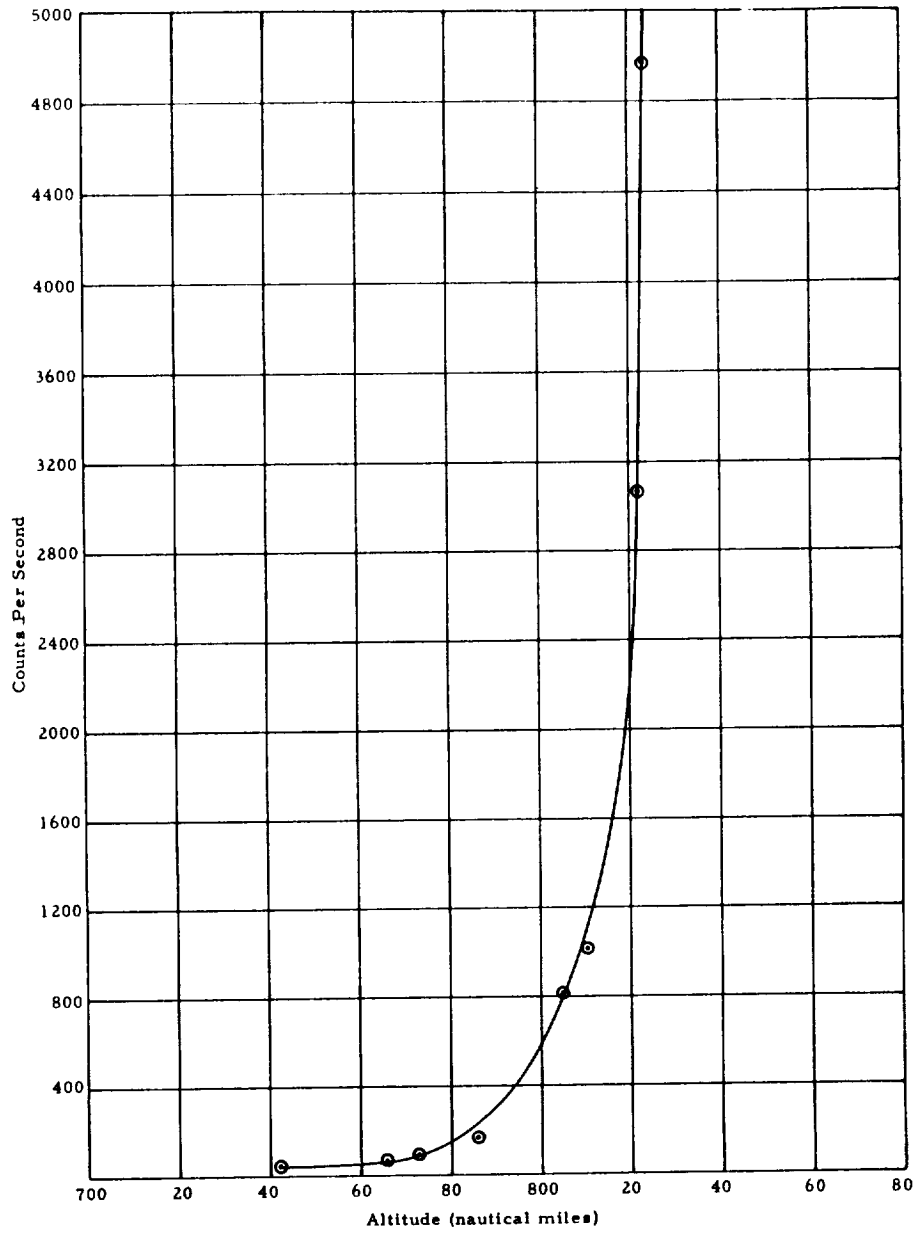


Figure 1-11. University of Chicago Proportional Counter Telescope Triples Rate.

b. In the altitudes ranging from approximately 2000 to 13,000 nautical miles, the radiation level is in excess of 2 roentgens per hour. This result yields a quantitative measure of the depth of the radiation belt in the region of 30-degrees north latitude.

c. In the vicinity of 20 degrees north latitude, the peak of the radiation belt occurs at an altitude of  $6000 \pm 1000$  nautical miles.

d. The maximum radiation level observed is 10 roentgens per hour. However, because there was an uncertainty in the chamber pressure, it is possible that this value is too low by 60 per cent.

e. A pronounced latitude effect is observed at an altitude of 1500 km. At  $25^{\circ}$ N latitude the radiation gradient is 0.2 roentgen per hour per degree change in latitude.

f. The count rate, as observed from the University of Chicago count rate telescope, increased in a manner similar to the increase in ionization. The average specific ionization was calculated from the omnidirectional intensity and the ionization level. The ratio of average specific ionization to minimum average specific ionization was found to be greater than 3. Since electrons of less than 1 mev cannot penetrate the walls of the ionization chamber, this high specific ionization could not be produced by 2 mev or greater electrons alone, but would require an admixture of electrons and protons.

g. Assuming that the flux consists of either electrons or protons or both, and that the primary ionization is greater than 20 ion pair/cm, then three possibilities exist.

(1) If only protons are present, their energy must be less than 70 mev.

(2) If only electrons are present, then their energy must be less than 0.05 mev.

(3) A mixture of both protons and electrons are present.

### 1.2.2.3.2 Inferences

On the basis of the evidence presented above, and from the data gathered thus far from the Explorer series of satellites, it is fairly well established that a great radiation belt exists around the earth, and that the radiation consists of charged particles temporarily trapped in the earth's magnetic field. Although the observations of Explorer and Pioneer were at the same latitude, they were at different longitudes. However, if the earth's magnetic field is the mechanism responsible for the trapping then the points of differing longitudes but similar geomagnetic latitudes should yield the same intensity of radiation. And if the geomagnetic coordinates are not known at these higher altitudes then it may be possible to make deductions regarding geomagnetic coordinates by comparing intensities. Simpson\* has pointed out that the effective geomagnetic equator for cosmic radiation is displaced by as much as  $45^{\circ}$  from the eccentric dipole field equator. It was thus of interest to compare the count rate of Explorer, which was located at  $80^{\circ}$  W longitude, with the count rate of Pioneer, which was located at  $20^{\circ}$  W longitude. Using the eccentric dipole model, the approximate location of the geomagnetic equator is at  $8^{\circ}$  S latitudes, for both the  $20^{\circ}$  W and  $80^{\circ}$  W longitude. Using Simpson's data for the cosmic ray equator, the geomagnetic equator is located at approximately  $8^{\circ}$  S latitude at  $80^{\circ}$  W longitude, and at approximately  $4^{\circ}$  N latitude at  $20^{\circ}$  W longitude. Thus, when Pioneer II was located at  $24^{\circ}$  N latitude, the corresponding angular distance from the geomagnetic equator would be  $32^{\circ}$  N geomagnetic latitudes according to the eccentric dipole field equator and only  $20^{\circ}$  N geomagnetic according to the cosmic ray equator.

A comparison of the count rate observed with the University of Chicago count rate telescope on Pioneer II with the Explorer IV geiger tube count rate yields the following indications. Under the assumption of an eccentric dipole model, the ratio of the omnidirectional intensity as determined from instruments on Explorer IV is greater than 4. On the other

---

\* J. A. Simpson, The Physical Review 102, 1648-1653, June 1953.  
 J. A. Simpson, Journal of Geophysical Research 61, 11-22, March 1956.

hand, if use is made of the cosmic ray equator then the ratio turns out to be approximately one. This result is then an indication that at altitudes of 1500 km the terrestrial geomagnetic field does not represent the field which is effective in the deflection of cosmic ray particles. It may thus no longer be possible to represent the field effecting cosmic particles by use of spherical harmonic analysis (i. e., a dipole model). Perturbation terms which are due to the effective currents of the particles trapped in the radiation belt, or possibly the solar magnetic field, may have to be added to the terrestrial eccentric dipole field.

#### 1.2.2.4 Magnetometer

Probing the distant geomagnetic field and testing for the existence of a lunar magnetic field is an area of vital interest to both geophysics and astrophysics. A rugged search coil instrument was chosen for this purpose since its sensitivity and simplicity are excellent.

##### a. System Description

The magnetometer consists of a search coil and a nonlinear amplifier which provides an appropriate signal to the telemetry channel. Upon installation in the vehicle, the coil is placed with the core lying along the circumference of the inner surface of the payload package in a plane perpendicular to the figure axis, and the core is bent to conform to the shape of the mounting surface. As the coil rotates with the vehicle, it experiences a change in flux through the coil as the aspect of the coil with respect to the magnetic field changes during the rotation. In a uniform and time-invariant magnetic field, the change in flux produces a sinusoidal voltage whose amplitude is proportional to the magnitude of the normal component of the magnetic field, that is, the magnitude of the component of the magnetic field in the plane perpendicular to the vehicle spin axis. In a time-varying magnetic field, the pure sinusoidal voltage has superimposed on it a voltage produced by the changes in flux arising from the time variations in the field. Figure 1-12 is a photograph of the package.

The magnitude of the magnetic field at the surface of the earth is 0.3 to 0.5 oersted, depending on the location of the point of observation. The magnitude of the field decreases roughly as the third power of the distance to the vehicle measured in units of the earth's radius. The field may therefore decrease to values as low as a micro-oersted. Since such an enormous dynamic range is clearly impractical for a linear amplifier, the magnetometer amplifier was made nonlinear. The resulting nonlinear amplifier covered a range of about three decades. The resulting instrument can measure fields varying from less than 6 microoersted to a value of 12 millioersteds. The upper limit is adequate to measure the normal component of the field at distances of roughly 1.5 earth's radii from the earth's center. The lower end of the scale was limited by noise, and so the minimum measurable value is slightly larger than would be ideally desired.

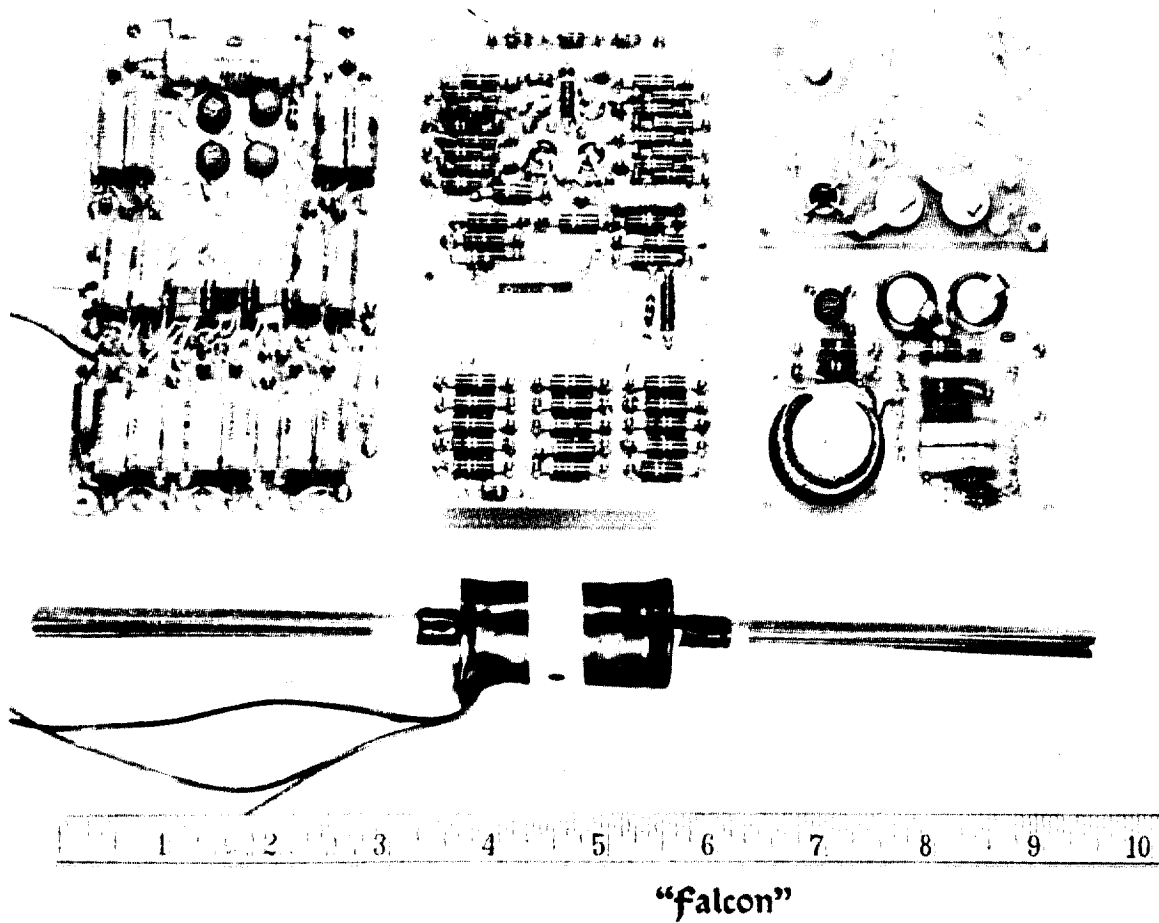


Figure 1-12. Magnetometer. Shown above is a front and back view of both the magnetometer amplifier and unbeamed oscillator as well as a search coil.

The nonlinearity of the amplifier was brought about by a feedback network. This feedback network resulted in relatively long attack and decay times for the amplifier. Because of the interesting transient effects observed on the flight of Pioneer I, the magnetometer supplied for Pioneer II used a second telemeter channel to transmit the variations of the amplifier AGC as well as the direct amplifier output.

b. Results

The data obtained from the magnetometer are exceedingly complex and are being statistically analyzed. Both quiescent field and transient effects have been observed. A computer program has been utilized to determine deviations from a theoretical model. An adjustment of the transmitter modulation deviation in the field resulted in a change in calibration increasing the error estimate of the quiescent field values obtained.

As seen in Figure 1-13, the general trend of the quiescent field follows that obtained by the theoretical analysis. Source scatter exists at the latter set of values. This is primarily a result of two effects: (1) the large dynamic range of the magnetometer amplifier tends to increase the absolute error, and (2) fluctuations in the data complicate the determination of the mean. (A computer program is being carried on to perform a complete statistical analysis.) The deviation of the field at 10 to 12 earth radii appears to have a real basis.

The deviation of the value of  $H_{\perp}^*$  from that based upon the model described can be attributed to several different effects, there being an error in the assignment of the position of the geomagnetic pole (for extreme altitudes), circulating current, or an increased energy density per unit volume of the geomagnetic field due to centrifugal forces acting upon an ionized medium into which is frozen the magnetic field.

Among the most interesting data are those concerned with fluctuations in field intensity. Since the search coil measures the component of magnetic intensity normal to the spin axis, changes in signal amplitude divorced

---

\*  $H_{\perp}$  is the magnetic field intensity perpendicular to spin axis.

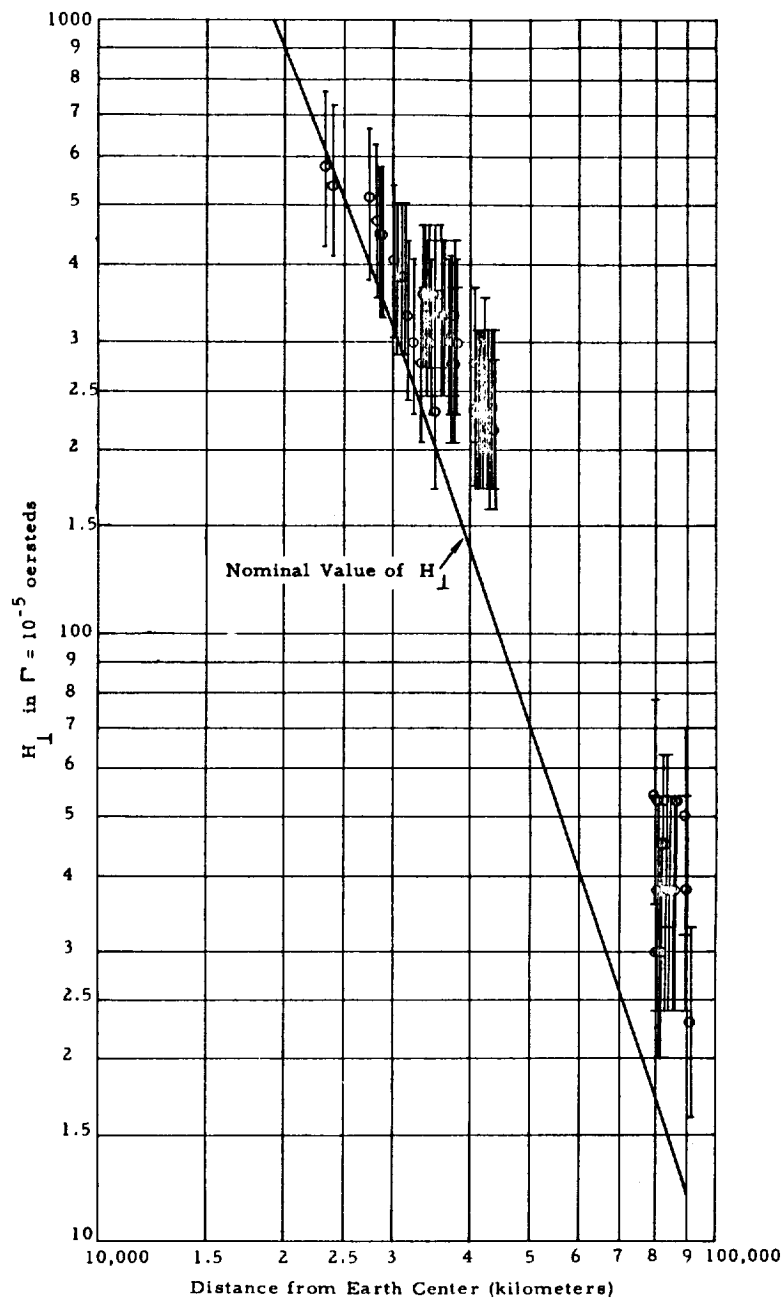


Figure 1-13.  $H_{\perp}$  Component of Magnetic Field in  $\Gamma$  vs. Distance from Center of Earth (Pioneer I). The nominal value of field plotted is the component normal to actual vehicle spin axis. The calculation is based upon the eccentric dipole model (see text) and the actual trajectory and attitude of vehicle in flight.



of phase changes, could be due to changes in the orientation of the direction of the magnetic field intensity in the polar sense (referred to the vehicle) and/or changes in magnitude. Over two hours of data taken in the region of 10 earth radii disclose many fluctuations in amplitude and apparently some in phase. The latter effect is seen by comparing the relative phase of the magnetometer sinusoid with that obtained from the r-f signal strength recording.

The following conclusions can be drawn from the preliminary analysis:

(1) Rotations of the magnetic intensity vector, through both large and small angles, appear. At least some of those associated with large angular excursions have characteristic times of the order of 10 seconds.

(2) Almost periodic oscillations in amplitude occur (sometimes accompanied by rotational changes) having lifetimes of 2 to 5 cycles and periods of the order of 10 seconds.

(3) The steady component of H, at 10 to 12 radii, has a magnitude several times that predicted by an eccentric dipole, thus suggesting the need for investigation of centrifugal instabilities in the terminal field, a possible modification of the present geomagnetic pole at extreme altitudes, or currents.\*

Generally speaking the magnetic field data is of considerable significance and a number of new effects have been observed. This flight provided an opportunity to make direct magnetic measurements on a scale intermediate between those found in the laboratory and those of truly cosmic size. The first direct look at magnetohydrodynamic events occurring on an enormous scale and detailed analysis of the data promises to be of great importance to a better understanding of astrophysical processes.

---

\* R. A. Helliwell has pointed out that very low-frequency Whistler-mode propagation would suggest a slight change in latitude of the geomagnetic pole.

#### 1.2.2.5 Micrometeorite Detector

It is of considerable scientific interest to observe micrometeorites at distances such that the earth does not block off nearly half the heavens and where the influence of the earth's gravitational field is considerably reduced. The micrometeorite experiment was essentially an attempt to make an initial survey of the number density and the rough momentum spectrum of micrometeorite particles at altitudes far above regions in which previous measurements had been made. A probe in orbit about the moon gives an opportunity to observe micrometeorite particles in a different gravitational field, and also a chance to study the effect of the moon in blocking the passage of particles from various directions in space.

In addition to statistics concerning the number of micrometeorites observed as a function of time and of vehicle position in space, it is of great interest to establish the characteristics of the individual particles. The Pioneer payloads contained a two-level detection system capable of separating the observed impacts into two classes which depend upon the momentum of the particle, a first step in measuring the momentum spectrum of the micrometeorites.

Early in the Able-1 program, the Air Force Cambridge Research Center was requested to assist in a micrometeorite experiment; the Geophysical Directorate of that organization had an extensive background in the field of micrometeorite research and had developed equipment which was applicable to the lunar probe program. AFCRC supplied the microphones for the detector, and the amplifier. In addition, it lent valuable assistance in the calibration of the micrometeorite system. The logic circuit was developed by STL.

Airborne components of the micrometeorite detection system consisted of (1) a detector (diaphragm and microphone), (2) a bandpass amplifier, and (3) two logic circuits (each with a trigger, flip-flop, and emitter follower). (See Figure 1-14.) The outputs of the logic circuits were fed to the subcarrier oscillators of the telemetry system. Figure 1-15 is a photograph of the equipment.

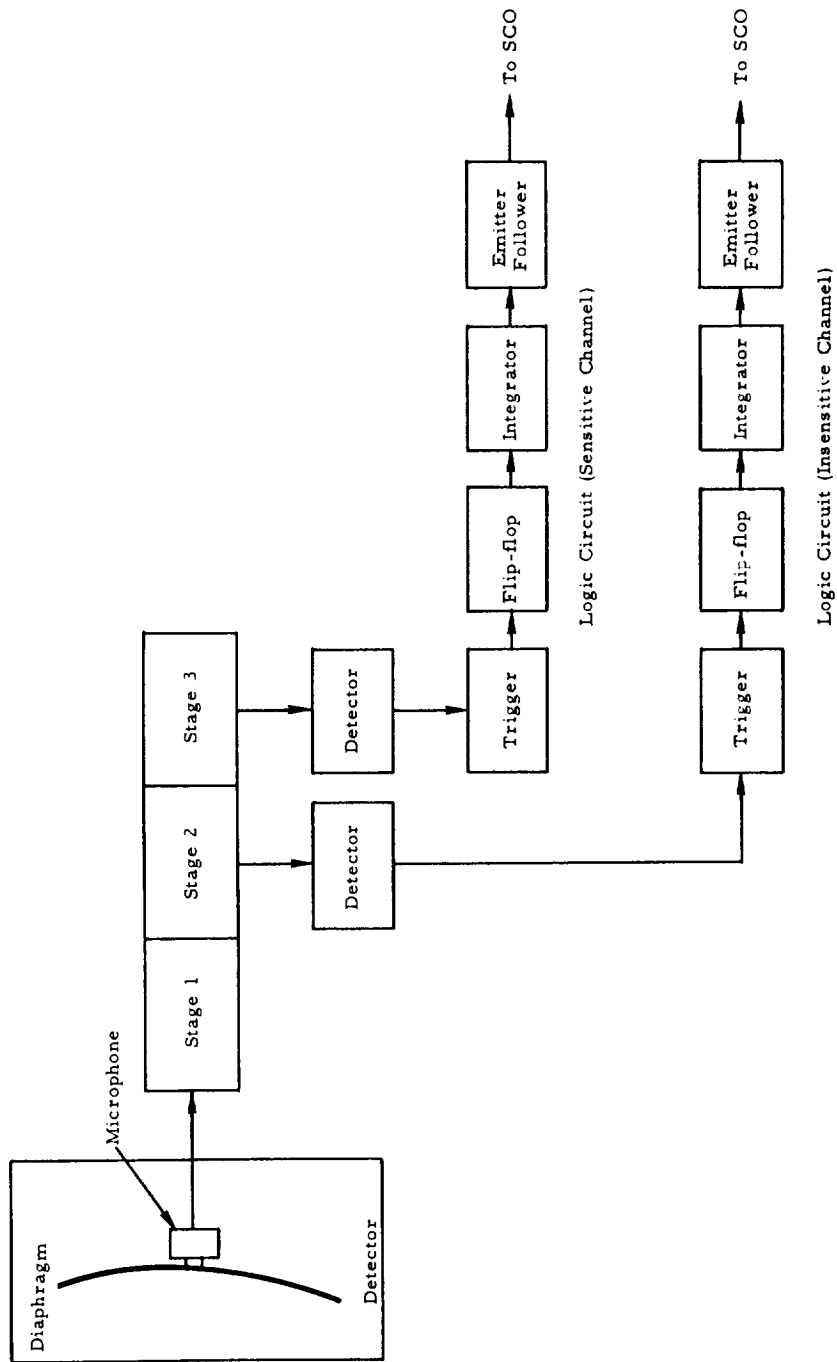


Figure 1-14. AFCRC Micrometeorite Detection System.

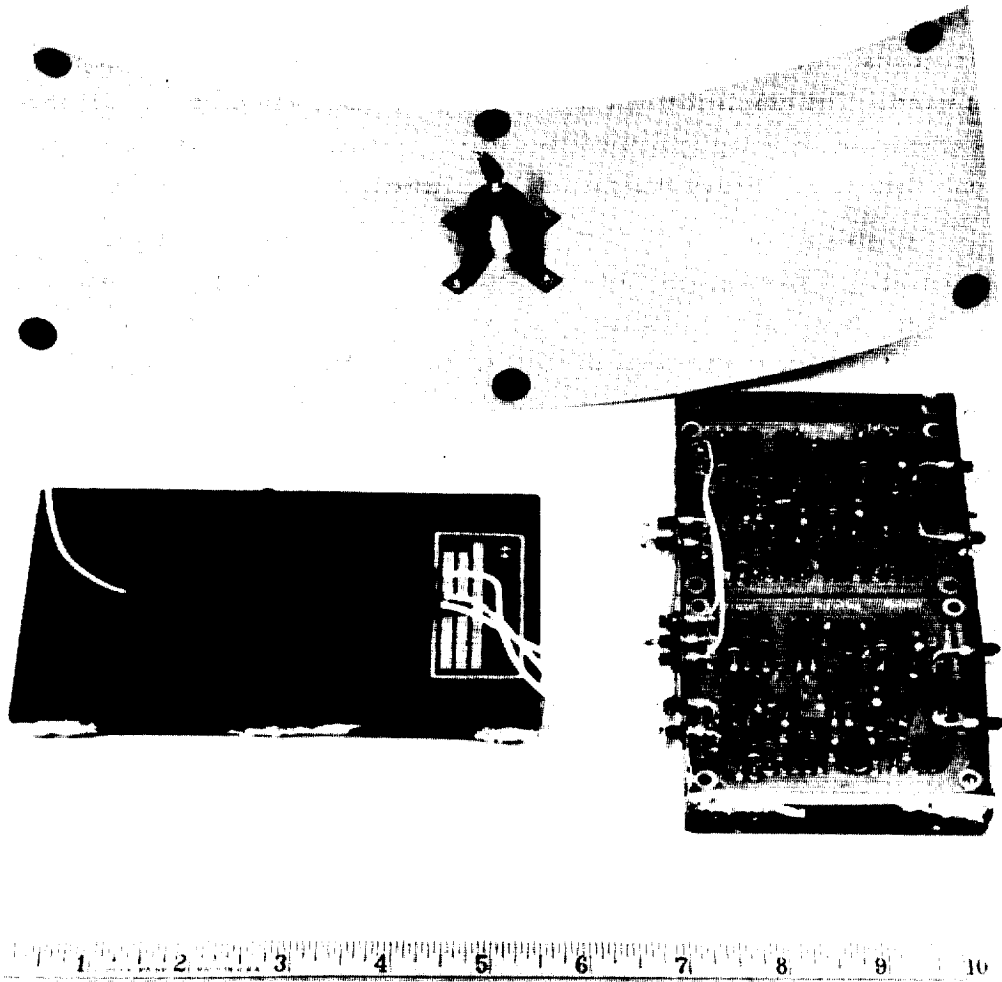


Figure 1-15. Micrometeorite Experimental Apparatus.

A micrometeorite striking the diaphragm generated an acoustic pulse which traveled through the diaphragm to the microphone. The microphone contained a piezoelectric crystal which rings at 100 kc under the influence of the acoustic pulse. The envelope decay time was approximately 3 milliseconds. The 100-kc signal was amplified in the bandpass amplifier and detected. The amplifier had three stages of gain; the output of all three stages drove the first logic circuit (sensitive channel), whereas the output from only two stages drove the second logic circuit (insensitive channel).

In either logic circuit, the input pulse (a replica of the 100-kc ringing envelope) was presented to a trigger. When the input pulse was greater than the trigger threshold, a sharp output pulse was generated. This pulse is used to change the state of the flip-flop (bistable multivibrator). The integrator was employed to reduce the rate of change of output voltage for later ease of data reduction. An emitter follower was employed to decouple the subcarrier oscillator from the logic circuit and to provide a low-impedance output.

When a small micrometeorite impacted on the diaphragm, a pulse existed at the output of two amplifier stages, but was too small to trigger the logic-circuit (insensitive channel). The same pulse existed also at the output of the third amplifier stage, but of larger voltage. When a sufficiently large micrometeorite impacted on the diaphragm, both logic circuits were triggered.

A surprising result of the Pioneer I flight was the paucity of impacts from interplanetary matter. The actual recorded strikes are shown in Figure 1-16 for the low momentum channel (No. 5) and in Figure 1-17 the single count observed on the high level subcarrier (No. 4). Since the area of the diaphragm was 0.0381 square meter and the number of low momentum strikes was 11 for the first nine hours, the mean flux over this time becomes  $9 \times 10^{-3} \text{ m}^{-2} \text{ sec}^{-1}$  in the momentum range of  $3 \times 10^{-4}$  to  $10^{-2}$  gram-cm/sec. The number of counts is sufficiently small so that detailed statistics are somewhat irrelevant. A general trend can be conjectured from the data, however; that is the flux seems to decrease away from the earth. The other pertinent comment is that only one count was

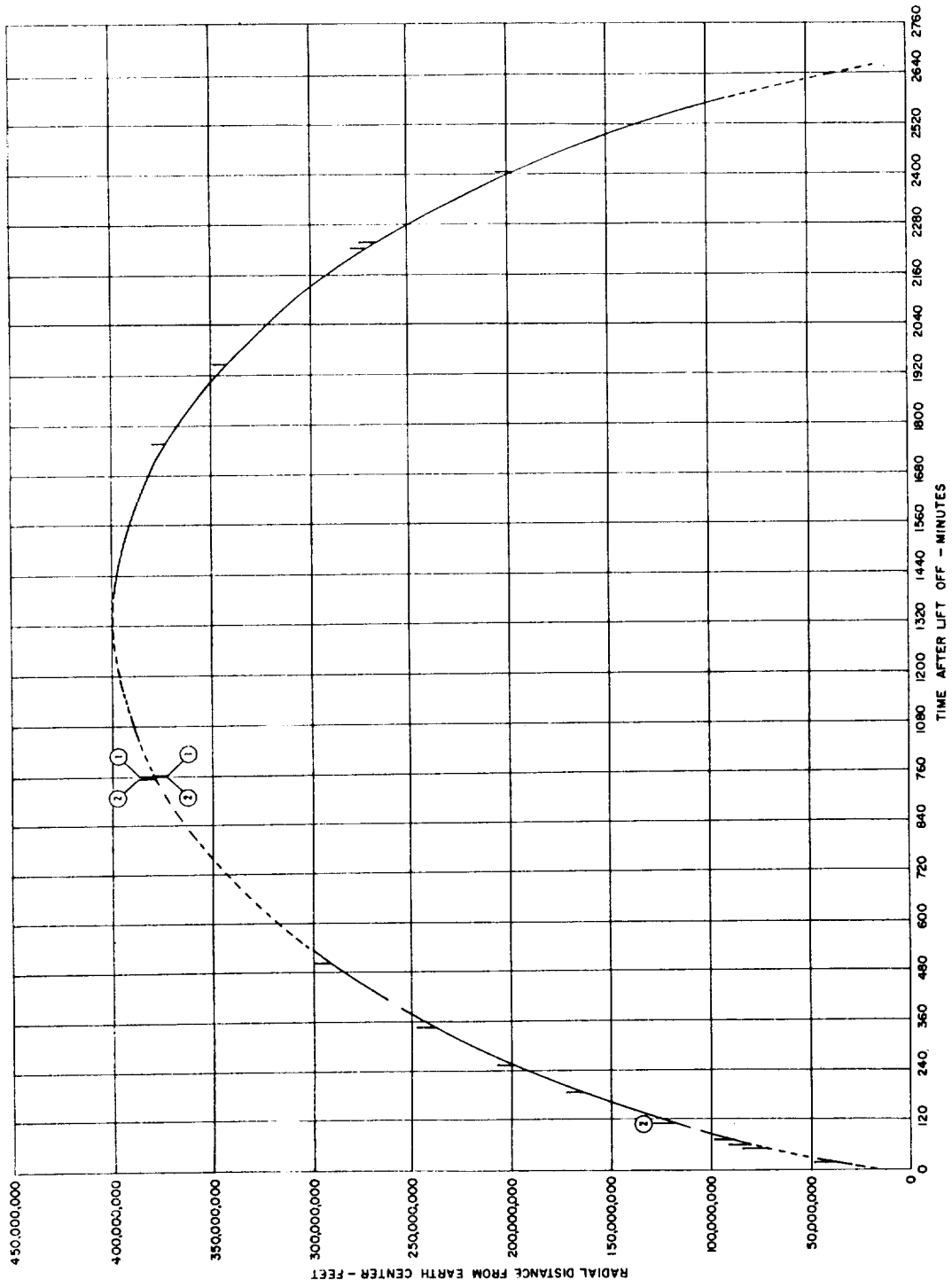


Figure 1-16. Micrometeorite Collisions Recorded by Low Momentum Experiment.

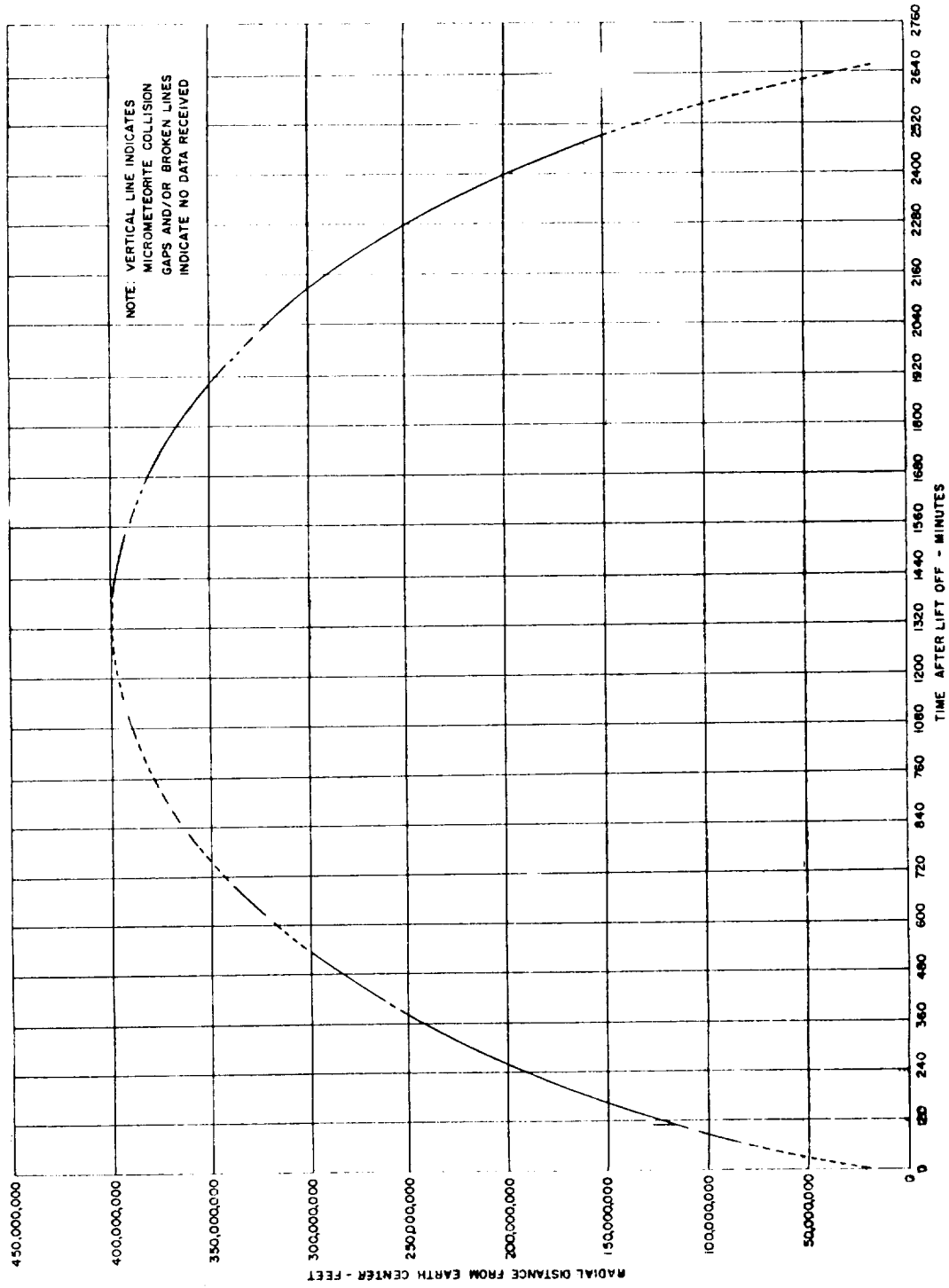


Figure 1-17. Micrometeorite Collision Recorded by High Momentum Experiment.

observed in the momentum class above  $10^{-2}$  gram-cm/sec, so that only a very general statement can be made to the effect that the flux does appear to grow with decrease in momentum.

On Pioneer II the results appear considerably different. Here the sampling is quite different in that the time interval was very short and the flux high. On the Malabar record at approximately 650 nautical miles altitude a strike occurred followed by three others within the following one minute of flight. The next receiver locked signal occurred at an altitude of 775 nautical miles. For the next one minute, 16 strikes were made indicating a burst of flux density  $6.1 \text{ m}^{-2} \text{ sec}^{-1}$ . In the ensuing short intervals of Manchester recording, no strikes were recorded. In the event that the count rate on Pioneer II is borne out by future experiments, the existence of an electromagnetic and/or a geogravitational containment of meteoritic debris about the earth is suggested.



#### 1.2.2.6 Temperature Measurement

Thermometers of two types were included in Pioneers I and II. These instruments were carried so that some estimate of the operating temperatures of the various pieces of equipment within the vehicle could be made. The temperatures recorded by these instruments are those of the elements themselves, and may be at some variance with the temperatures of other components in the package. The possibility of discrepancy stems from the fact that thermal equilibrium is attained by radiative processes since conductive and connective processes are not present, the components being separated by insulating materials and a vacuum.

Of the two thermometers, one was a thermistor, the resistance of which controlled the frequency of a subcarrier oscillator. The thermistor was mounted on an insulator inside the vehicle. The second was an electronic circuit the output of which, with constant voltage input, varied with temperature. The output of this circuit was also used primarily as a calibration voltage for the ionization chamber experiment.

The temperature of the thermistor during the flight of Pioneer I is shown in Figure 1-18. The temperature indicated by the ionization chamber calibration was about  $50 \pm 10^\circ\text{F}$  at 19 minutes after launch and had dropped to a value below  $32 \pm 10^\circ\text{F}$  after two hours. The low temperature readings of the latter device are based upon an extrapolated calibration, however, and are not reliable. Over the first two hours of the flight the temperatures as measured by these two devices agreed within approximately  $10^\circ\text{F}$ . The values indicated by the ion chamber calibration pulse for later times were not included on the calibration curves, thus necessitating extrapolation.

For Pioneer II the temperature history of this flight, as measured by the thermistor, is shown in Figure 1-19. The temperature, as indicated by the calibration pulse, remained approximately constant at  $68 \pm 5^\circ\text{F}$  over the first 15 minutes of the flight.

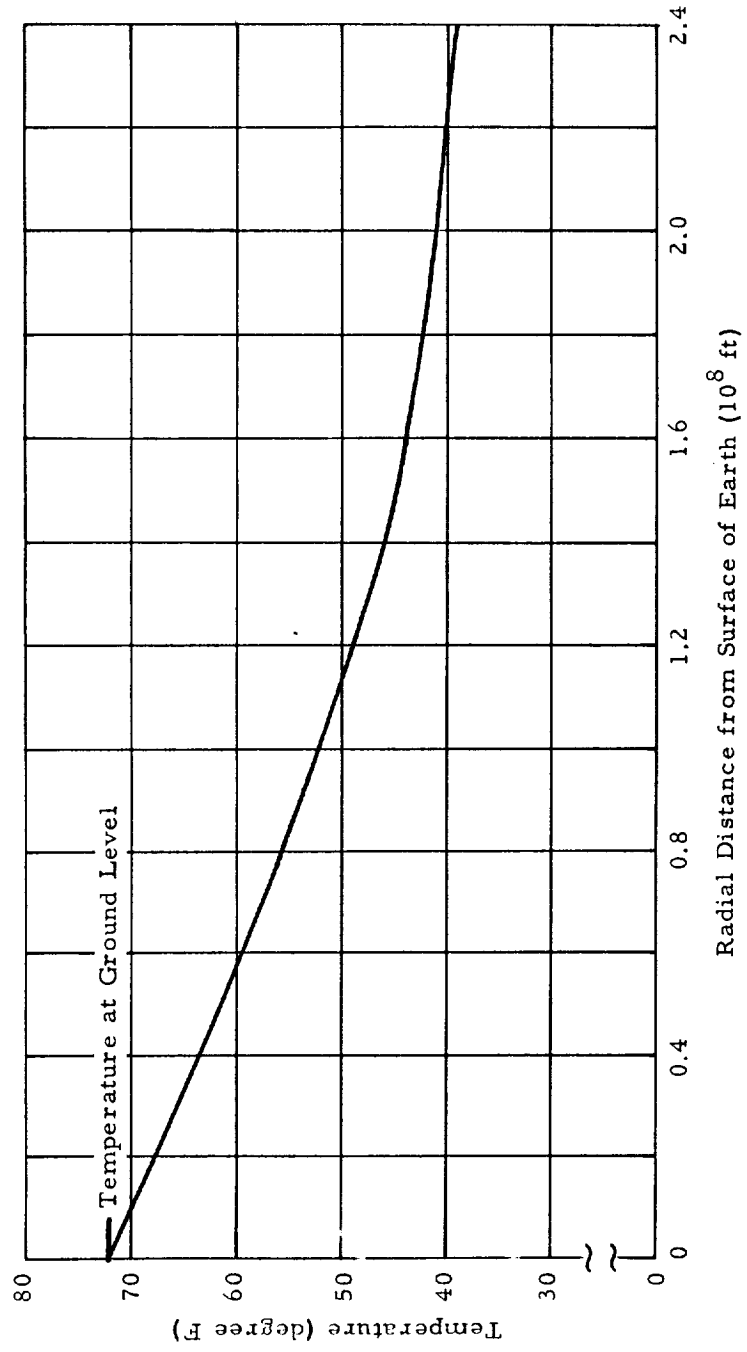


Figure 1-18. Temperature Versus Radial Distance from Earth's Surface for Pioneer 1.

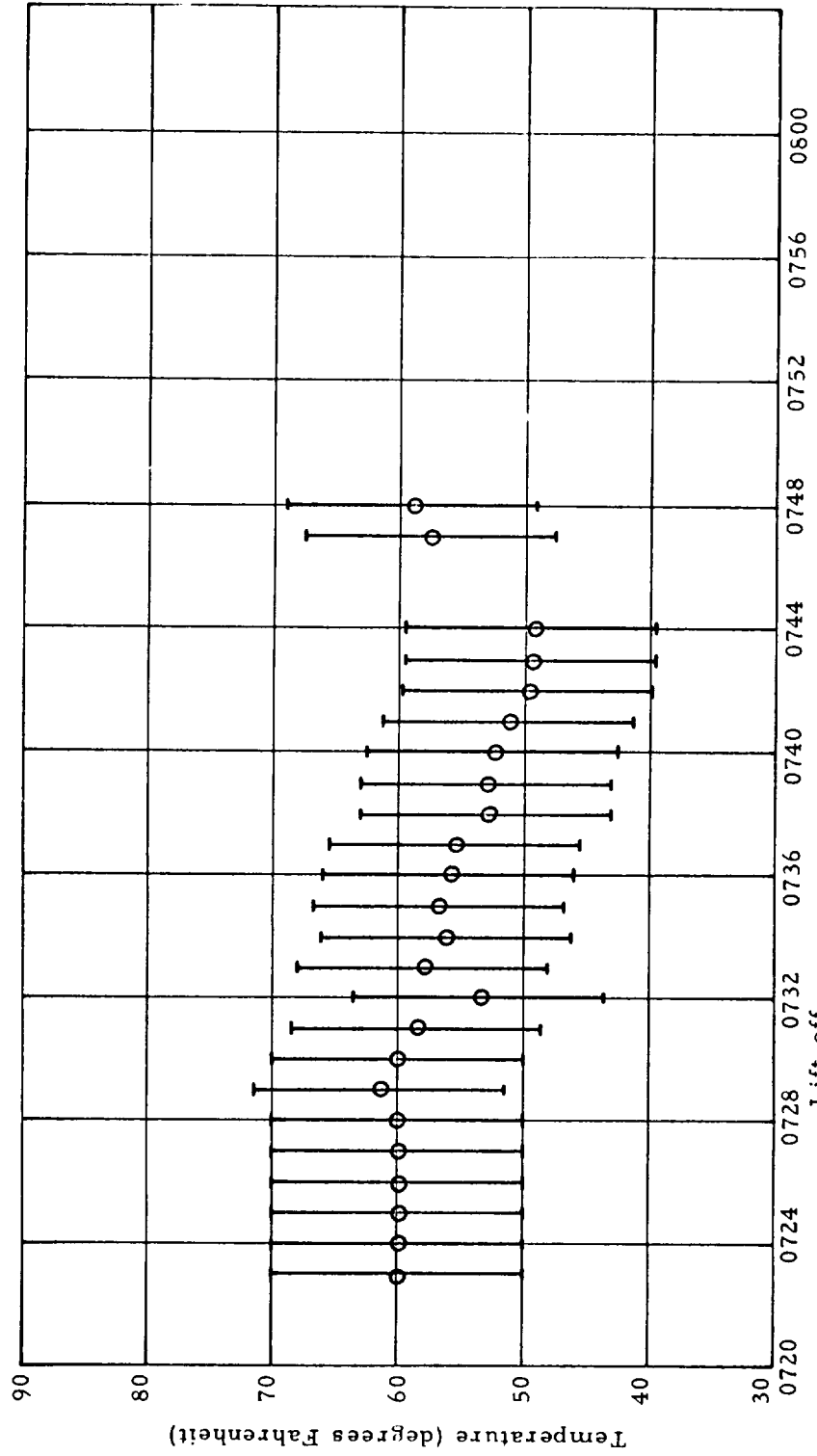


Figure 1-19. Temperature History of Pioneer II.  
Greenwich Mean Time (7 November 1958)

#### 1.2.2.7 STL Television

The payload on the last flight contained a television system for the purpose of obtaining a rudimentary image of that part of the lunar surface normally unseen by earth observers.

The system was designed to utilize vehicle motions to accomplish both line and frame scanning. A nominal output bandwidth of 1 cps was provided in order that the microlock telemetry link could be employed to transmit the image information to earth. The system had an optical resolution of 0.5 degree; a single scan line contained 126 resolvable elements.

Figure 1-20 is drawn to illustrate system operation. An optical unit, containing a concave spherical mirror which reflects light on a photosensor, is fixed within the vehicle. Light arriving within an acceptance cone, or optical beam of 0.5 degree (total angle), causes the voltage of the sensor to increase.

As the payload rotates and moves forward along its trajectory, the optical beam scans a cylindrical helix in space. Over a small area of this helix, line scanning is produced by vehicle spin and frame scanning by vehicle motion along the trajectory.

When the optical beam is scanning empty space, the photosensor output is zero. When a beam scan intersects a bright object in space, such as the earth or moon, the photosensor output voltage at any instant is proportional to the average brightness of the area seen by the optical beam. As the beam travels across the surface of the planet during each spin revolution, a video waveform is generated. The electrical bandwidth required to transmit this video signal is about 1 kc.

The electronic circuitry of the TV system is employed to reduce the bandwidth required to transmit the video signal. Bandwidth reduction is accomplished in a manner explained below.

A 64-degree line segment of each scan revolution is chosen for transmission. The beginning of the line is made to correspond to the limb of the

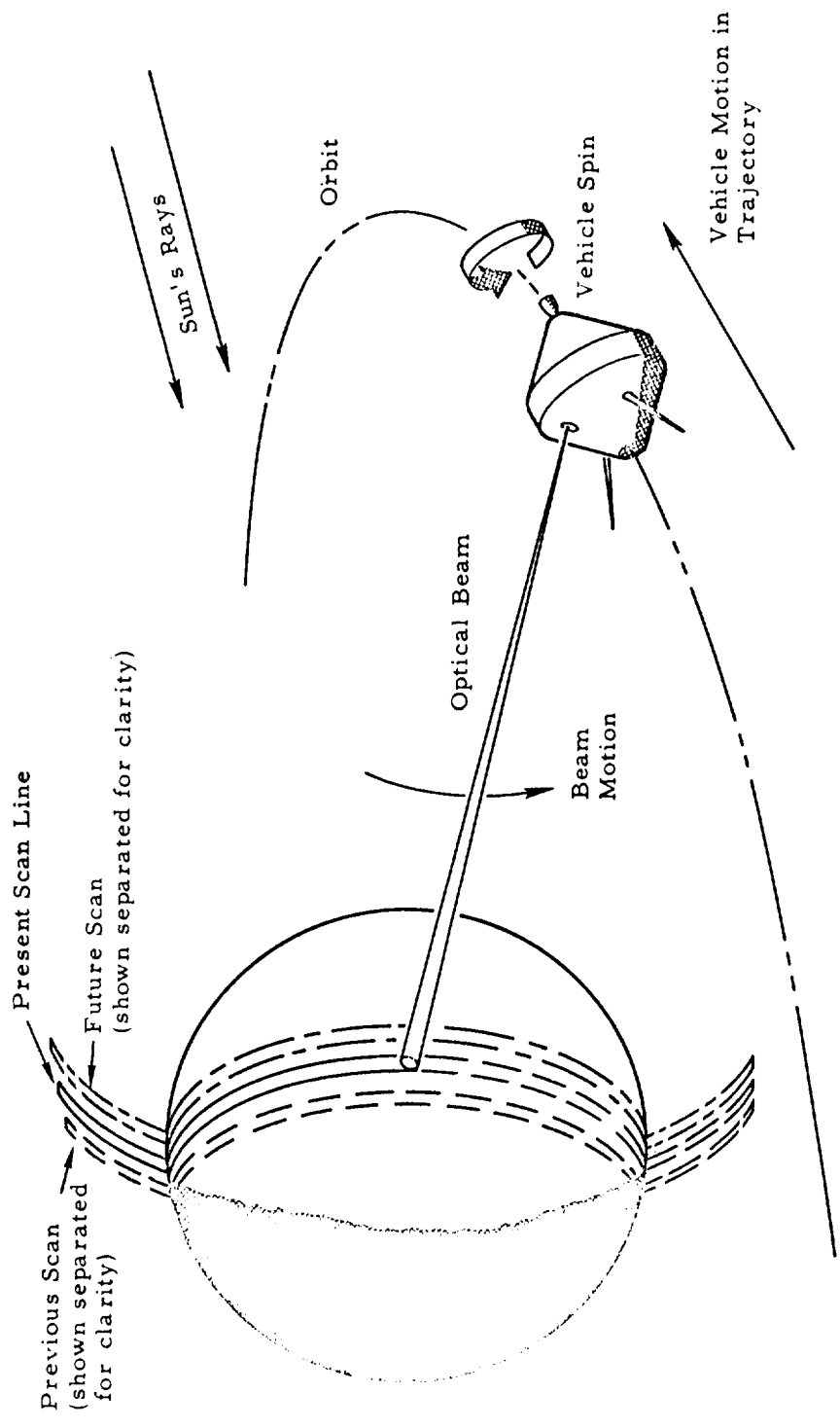


Figure 1-20. Illustration of TV System Operation.

planet being scanned. Each scan line is divided into 128 successive elements, each element about 0.5 by 0.5 degree, corresponding to the optical bandwidth. Only one element is sampled during each spin revolution, so that 128 revolutions are required to obtain a single 64-degree scan line. Successive elements along a scan line are obtained each spin revolution by sampling the video waveform at successively more delayed times from the waveform beginning. The sampling scheme is illustrated in Figure 1-21.

The amplitude of the sample is proportional to the instantaneous brightness of the planet surface at the time the sample is taken. The sample amplitude is held and transmitted over the telemetry system during the remainder of each spin revolution. In this manner, only two samples, or elements, of the image are transmitted each second (for a 2-rps spin rate) which reduces the minimum video bandwidth to 1 cps. The video waveform is, effectively, "stretched."

No flight data were obtained from Pioneer II due to the brevity of the flight, and the fact that most of the earth scanned was in darkness.

The TV system provided for Flights 1 and 2 by the Naval Ordnance Test Station is not discussed here since NOTS will provide a separate report on this equipment.

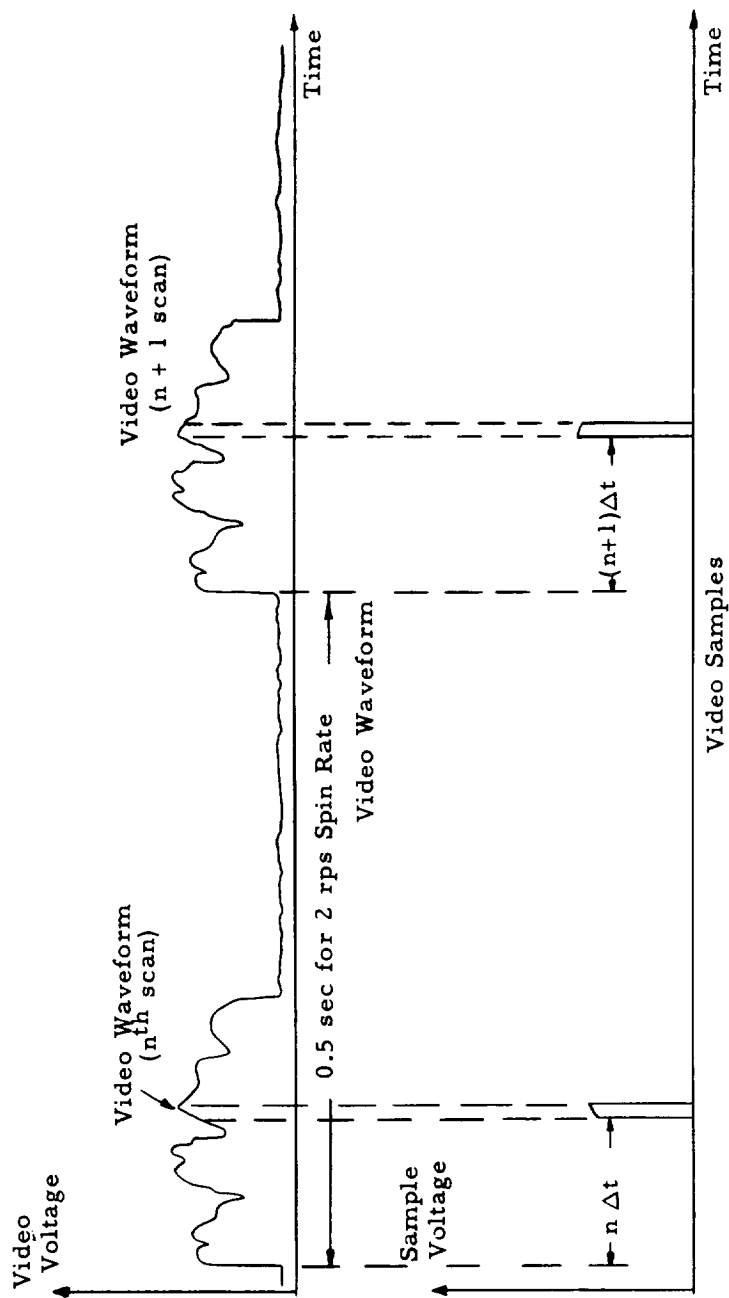


Figure 1-21. Sampling Scheme Shown for Two Spin Cycles.

### 1.2.3 Telemetry

#### 1.2.3.1 Transmitters

A 300-mw transmitter operating at a frequency of 108.06 mc was used in Flight 2 for both telemetry and doppler information. Normally telemetry information was transmitted, but on command from the ground the transmitter functioned as the return link of the two-way coherent doppler system (see Section 1.2.4). On Flight 3 a 100-mw r-f oscillator operating at 108.09 mc was added to supply telemetry during doppler interruptions and redundant telemetry at other times. Both transmitters were phase modulated by a complex subcarrier spectrum applied through a multiplexing amplifier which summed the outputs of the various subcarrier oscillators.

The system was designed to yield a signal-to-noise ratio of 10 db over a 10-cps passband. An isotropic transmitting antenna was used.

#### 1.2.3.2 Subcarrier Oscillators

Each of the experiments on Pioneer I was fed to the input of a subcarrier oscillator. The five subcarrier oscillators carried in Pioneer I corresponded to the first five RDB standard channels beginning with 400 cps and ending at 1300 cps center frequency. Guard band specifications for the RDB standards were observed. Channel 1 contained ion chamber information, Channel 2 magnetometer data, Channel 3 temperature data, and Channels 4 and 5 micrometeorite data. The output of each of the subcarriers was an audio tone whose frequency was dependent upon the input signal and therefore upon the physical information. The subcarrier spectrum was then summed into the multiplexing amplifier so that a composite was obtained which was used to modulate the transmitter. Design criteria indicated that the rms value of the phase deviation of the transmitter signal should not exceed 30 degrees.

For Pioneer I the total signal spectrum consisted of a carrier and of five side-band pairs totaling 11 spectral lines. Eighty per cent of the power was contained in the carrier frequency and 4 per cent of the power in each of the side-band pairs, so that the subcarrier complex contained 20 per cent of the total transmitted power.



In Pioneer II, six subcarrier channels were used. Channel 1 carried ion chamber information. Channel 2 carried the magnetometer note. Channel 3 carried the STL television signal. Channel 4 consisted of two multiplexed pieces of information--the micrometeorite total count rate and temperature data. (The two-level micrometeorite momentum spectrometer was abandoned for this flight because of the lack of telemetry capacity within the six sub-carriers.) Channel 5 carried the signal rate on the triple-coincidence proportional counter telescope, and Channel 6 the triples rate which was multiplexed with the AGC voltage from the magnetometer amplifier. The AGC voltage was transmitted to increase the range over which the magnetometer could be read, since the AGC signal was a more slowly varying function than the 2-cps note.

Final adjustment of the telemetry system and study of the subcarrier oscillators took place at Cape Canaveral, AFMTC. The final check of the system was done with the fourth-stage payload mounted in place, the signal being read off an r-f link to the fourth-stage telemetry doppler. Each of the experiments, in turn, was activated--the magnetometer by a bar magnet, the micrometeorite by striking the diaphragm, and the radiation experiments by means of a Cobalt 60 source. In addition to preparations, final calibration of the sensors for the third flight took place at AFMTC in the payload laboratory.

#### 1.2.3.3 Data Collection for Flight 2

The telemetry on Flight 2 was designed to function over all flight intervals and was limited only by doppler breaks and lock time from the various stations. During the first 17 minutes of this flight, the doppler lock removed the subcarrier modulation from the transmitter. At T plus 17 telemetry was activated and signals were received at Manchester. Due to the deviation in the flight path of the vehicle, the antenna tracked on a side lobe for the first hour. Estimates of the side lobe degradation vary from 30 to 40 db. The result was loss of lock for a good portion of the first hour's flight. However, sufficient lock time occurred to enable radiation measurements to be made from about 2000 n mi on. Magnetometer data were irregular, apparently because of the faulty subcarrier oscillator.

Overlap as planned occurred between Hawaii and Manchester. Much of the loss of a signal in the initial hour can be attributed to the number of doppler commands. Total time of telemetry reception for the various channels is shown in Figure 1-22.

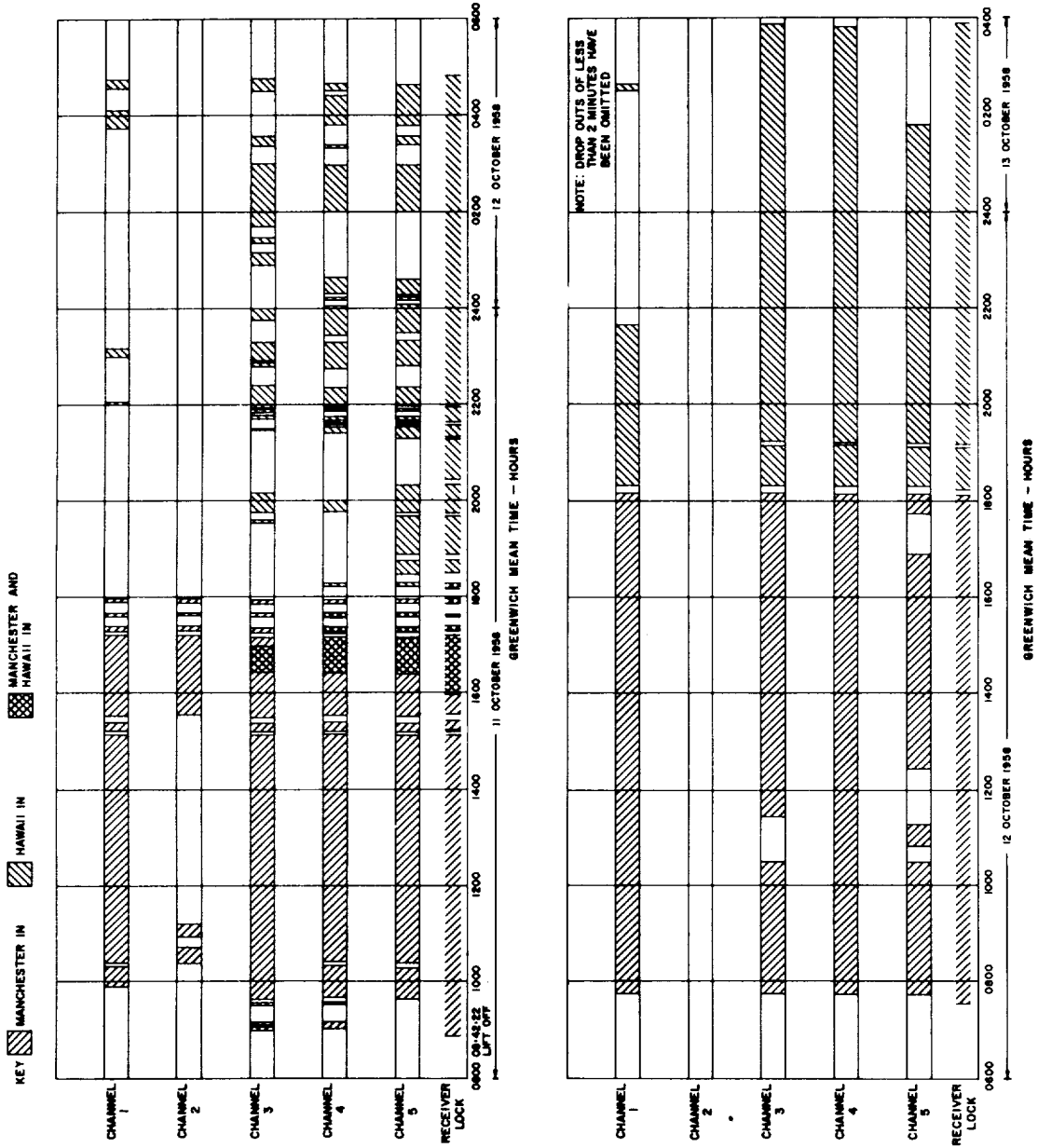


Figure 1-22. Telemetry Reception at Various Stations (Flight 2).

#### 1.2.3.4 Data Collection for Flight 3

The principal receiving sites for Flight 3 were Manchester, ABAMA-Hold (located at AFMTC), NRL (AFMTC), and Radiation, Inc. at Malabar, Florida. All six subcarrier channels except the No. 3 television channel showed data. The television was blank because of the vehicle's position in the earth's shadow for all except the last portion of the flight, at which time the vehicle was below the horizon for all stations.

Manchester data were limited to short segments because of the low apparent altitude of the vehicle as seen by Manchester. This low look-angle resulted in serious multipath problems and consequent excessive fading and loss of receiver lock. The data have been exhaustively checked for receiver lock, and it is believed that all regions of lock have been demodulated. Some further work on the tapes is being done, especially to check Channel 6, the proportional radiation counter singles rate.

#### 1.2.4 Command/Doppler System

##### 1.2.4.1 General

Because the preliminary plans for the Able-1 program did not provide for vernier adjustment of the burnout velocity and because the retrorocket was to be triggered by a timer set before launch, calculations performed in April showed that the probability of vehicle capture by the moon's gravitational field would be only about 30 per cent. In order to increase the capture probability, a measurement of the radial velocity was required. To permit velocity adjustment and retrorocket firing upon command from the ground, the decision was made during the latter part of April to employ a doppler transponder and command receiver. Work on the design of such a system was begun on 1 May 1958, with a goal of incorporating it into the first Able-1 shot by the middle of August. All the work described in these sections was done in about three months and finished in time for the first lunar probe shot on 17 August 1958.

The primary purposes of the Doppler and Command Link were (a) to determine radial velocity of the vehicle to a high accuracy in order to permit the firing of the correct number of vernier rockets and in order to help determine the accurate time of retrorocket firing, and (b) to communicate to the vehicle commands regarding vernier firing, vernier structure staging, and retrorocket firing. A secondary purpose of the link is the measurement of range.

Various constraints were imposed on the development of the Doppler and Command Link. As far as the airborne equipment was concerned, weight, size, and power consumption were of primary importance. The available electronics payload was allocated to various scientific experiments, and less than 10 pounds was available for the required receiver and transmitter. A similar stringent limitation was imposed on the available space and power. A simple antenna configuration had to be used, both for received and transmitted signals. The limited time available made it mandatory to use as many existing and available components and proven techniques as feasible. Since some of the ground equipment was already either in existence or on order, including Microlock receivers and a large receiving antenna, the

system was designed to simplify the airborne package which had to be designed, breadboarded, and manufactured within an extremely short time. A powerful ground transmitter, which could be purchased and installed within a short time, was one of the items which permitted some simplification of the airborne equipment.

Figure 1-23 is a simplified block diagram of the doppler transponder and command receiver system. Figure 1-24 is a photograph of the completed airborne unit.

#### 1.2.4.2 System Characteristics

Because the vehicle was spin stabilized and because of the wide range of aspect angles over which the system must function, the payload antenna had to be very nearly isotropic. To avoid amplitude and phase modulation of the signal received by the ground tracking station, the polarization characteristics of this antenna had to be symmetrical about the spin axis. The antenna selected was a simple axial dipole, used for both transmission and reception. At the primary ground station in Hawaii the Air Force made available a fully steerable 60-foot parabolic dish with a gain of about 24 db at 108 megacycles per second which was used for reception. A helix of approximately 14-db axial gain was employed for transmission. Both transmitting and receiving ground antennas are circularly polarized. The antennas used for transmission and reception at AFMTC are 14-db helices identical to the transmitting helix at the Hawaii station.

The power of the ground transmitter in Hawaii was 5 kilowatts. The airborne transmitter developed was a completely transistorized unit with an output power of between 300 and 500 milliwatts (adjustable); 400 milliwatts is specified for normal operation. The IGY frequency of 108 megacycles per second for the air-to-ground transmission was used. At a range of 240,000 miles and with the available transmitter powers and antenna gains, the signal power at the airborne receiver is about -110 dbm and that at the ground receiver in Hawaii is approximately -139 dbm. Operating at these signal levels required use of receivers with extremely narrow effective bandwidths. Although a suitable receiver was available for the ground stations (i. e. the Microlock tracking system), no receiver

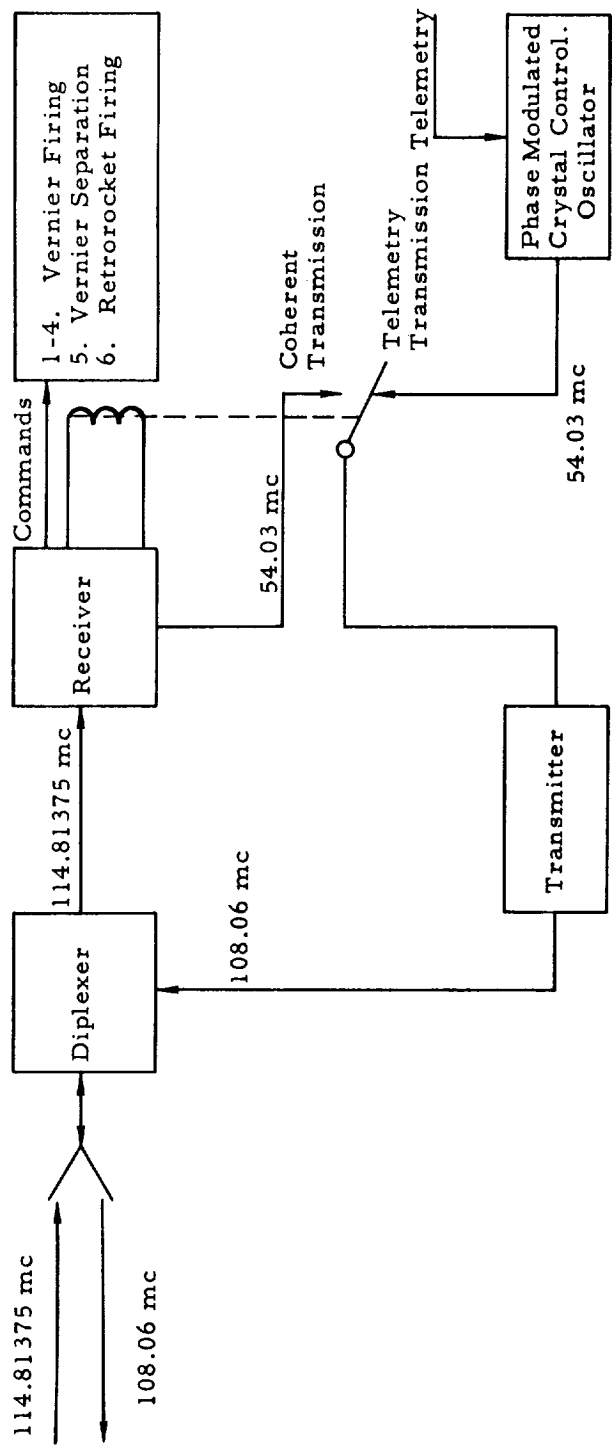


Figure 1-23. Simplified Block Diagram, Doppler Transponder and Command Receiver.

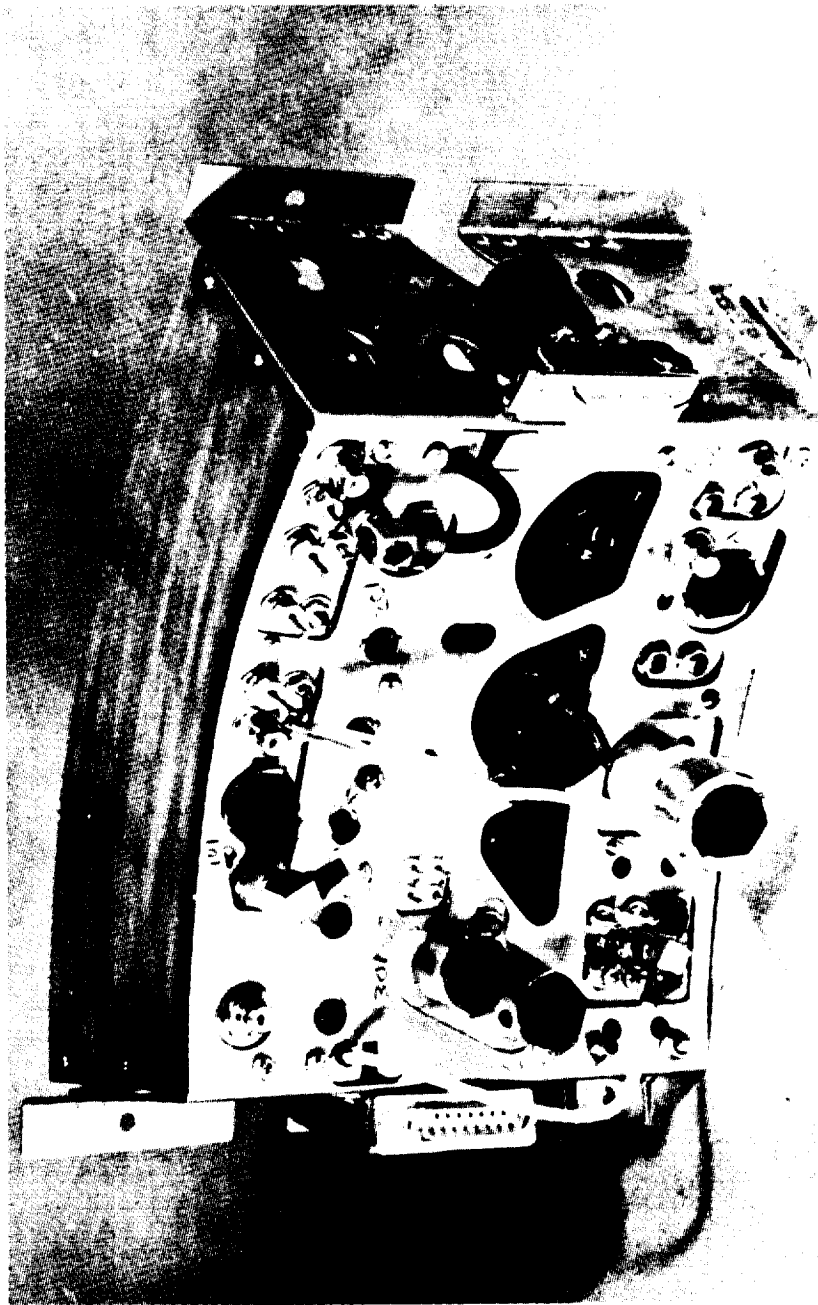


Figure 1-24. Doppler and Command Receiver.

existed which could be modified or adapted for use in the airborne subsystem. Therefore, STL had to undertake development of an extremely sensitive transistorized and ruggedized receiver for incorporation in the payload package. The only receiver type meeting these requirements was the phase-locked receiver with an equivalent noise bandwidth of a few hundred cycles per second.

Because the airborne subsystem has to be capable of functioning as a coherent doppler transponder, for the sake of transmitter-receiver isolation it was essential to provide a method of coherent frequency offsetting or conversion. The method employed for the generation of this coherent frequency offset is illustrated in Figure 1-25. It will be seen from this figure that the output of a voltage-controlled oscillator (VCO) at the intermediate frequency is multiplied by a factor of 16 to obtain the local oscillator signal. The frequency of the voltage-controlled oscillator is controlled by means of an error signal generated by phase detecting the output of the IF strip with respect to the signal from the VCO.

As shown in Figure 1-25, the local oscillator signal is then amplified and transmitted to the ground system. With the configuration illustrated, the operation of the receiver is such that the frequency of the signal retransmitted by the transponder is precisely  $16/17$ ths of that received. Thus, a 108-megacycle per second signal radiated from air-to-ground corresponds to a ground-to-air frequency of 114.75 megacycles per second and to an intermediate frequency of 6.75 megacycles per second.

In order to extract the doppler data at the ground station it was necessary, in essence, to generate a reference signal at  $16/17$ ths the frequency of the transmitted signal and to beat this signal against the signal received by the Microlock receivers.

Commands were encoded onto the ground-to-air signal by phase modulating the transmission with audio frequency tones whose frequencies are considerably higher than the bandwidth of the phase-locked loop. The well-known device of employing a coincidence of multiple tones was employed, here two. Provision was made for a total of four tone channels, with tone frequencies of 2000, 2500, 3000, and 3500 cycles per second. The



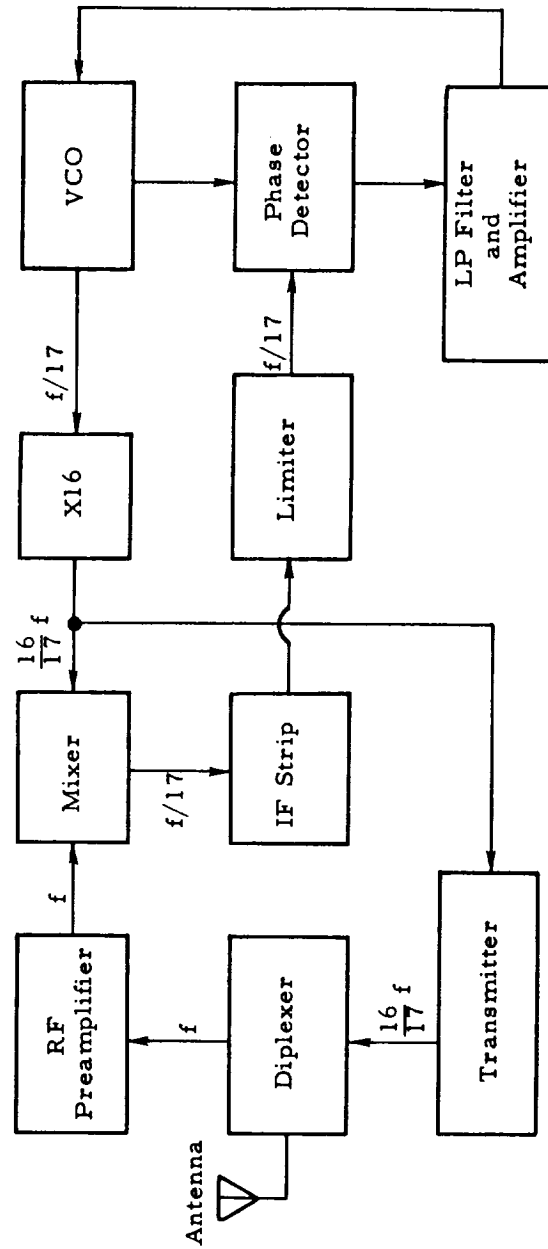


Figure 1-25.. Basic Airborne Phase-Locked Loop and Transponder.

bandwidths of the audio tone filters were specified as 50 cps.

The noise bandwidth of the Microlock receivers in the ground system is approximately 20 cycles per second. With this bandwidth and with a total noise input (galactic noise plus receiver noise) equivalent to that produced by a receiver with a 6-db noise figure, these receivers maintain lock down to a signal level of -150 dbm. Since the power received from the 400-milliwatt airborne transmitter would have been about -139 dbm at Hawaii when the payload package was in the neighborhood of the moon, the transmitted power should have provided a margin of approximately 10 db over and above the power required by the Microlock receivers to maintain marginal lock.

The noise bandwidth of the receiver as presently designed is approximately 150 cycles per second at a signal level of -130 dbm. With this bandwidth and with a total noise input equivalent to that produced by a receiver with a 10-db noise figure, analysis indicated that the receiver should be capable of locking onto the received signal down to signal levels of between -130 dbm and -140 dbm. A design objective of -130 dbm was chosen for lock-on and command channel operation, while operation at -120 dbm was regarded as an acceptable performance level. Since the received signal power in the neighborhood of the moon should be about -110 dbm, these figures correspond to a desired operating margin of 20 db, with a 10-db margin required.

In order that the airborne equipment could operate unattended, the system contains a number of auxiliary decision-making features.

Since the rapid pull-in range of the phase-locked loop in the airborne receiver was very considerably less than the uncertainty in the frequency of the received signal, it is necessary to provide the loop with an auxiliary acquisition circuit. When the loop sweeps past the frequency of the signal, a bias voltage is generated which effectively counteracts the sweep voltage. After a delay of a fraction of a second, this dc bias voltage serves to trigger the threshold circuit and thus to disconnect the sweep circuit. The period of the acquisition sweep is set at between 6 and 10 seconds and the threshold level is set just high enough so that excessive false triggering does not occur. The lower limit of a 100-cycle per second loop bandwidth

permits a reasonable sweep time.

In addition, since the time during which the airborne system actually receives a signal from the ground transmitter is very small relative to the length of the time over which the receiver must operate, it was necessary to provide the command channels with additional protection against false triggering by noise, over and above that provided by their coincidence and threshold circuitry. For this purpose a signal-present circuit is employed. The output of this circuit is fed to a threshold detector which when triggered, enables the command channels.

Low-frequency noise in the phase detector output is effectively removed by the low-pass filter and, by virtue of the action of the limiter, the threshold detector serves to make a decision that, first, the loop is locked, and second, that the input signal-to-noise ratio is sufficiently high to warrant enabling the command channels. To provide an additional measure of protection against interfering signals and noise, provision was made to disable the command channels immediately whenever the acquisition circuit resumes sweeping.

In the interest of simplicity and economy of size, weight, and power, the same transmitter was employed both for telemetry transmission and for transponding the doppler signal. Another telemetry transmitter was added in Flight 3. In the normal mode of operation a quartz-controlled exciter is modulated by telemetry subcarriers and fed into the transmitter whenever a signal is not being received from the ground transmitter. When the loop is locked, as indicated by the signal-present signal, the exciter with its telemetry modulation is disconnected and the transmitter is connected to the output of the receiver local oscillator.

#### 1. 2. 4. 3 Final Performance Characteristics

The completed receiver showed a signal lock-on capability of about -130 dbm. Commands could be transmitted and correctly decoded at about -127 dbm consistently.

The period of the acquisition sweep was 7.5 seconds, and included time for sweeping the expected frequency range plus a guard band at either end.

The total power consumption when acquired was 270 milliwatts and when sweeping 215 milliwatts, an extremely low power drain considering that the receiver alone contained 72 transistors. The battery weight for the receiver, based on 120 hours of operation for the cells of highest drain, came to 1.56 pounds.

The weight of the receiver, including batteries, came to 5.7 pounds and the total volume came to 90 cubic inches.

### 1.3 Vehicle Characteristics

The Thor Able-1 is a four stage vehicle consisting of three booster stages and a terminal stage composed of eight vernier rockets, an orbit injection rocket, and a payload. Interstage structural attachments between successive stages are provided with means for in-flight separation. A nose fairing, jettisoned during second-stage operation, covers the third and fourth stages.

#### 1.3.1 Trajectory Considerations

The powered and free-flight trajectory was selected to maximize the probability of lunar capture for the expected vehicle dispersions considering several constraints:

- a. The retrorocket attitude and the third stage attitude are the same in inertial coordinates.
- b. At the time of nominal retrorocket firing, the vehicle should be well above the horizon of Hawaii (preliminary trajectory analysis indicated that the command transmitter for retrorocket firing should be located at Hawaii).
- c. The payload capability of the vehicle should be reduced only a little.
- d. The relative velocity of the vehicle with respect to the moon had to be low enough so that the approximately 2800 ft/sec increment imparted by the retrorocket would result in capture.

Computer studies revealed that a free-flight trajectory with an initial flight path angle with respect to the local vertical of approximately  $70^{\circ}$  and an energy corresponding to a velocity of approximately 35,400 ft/sec at an attitude of 200 miles satisfied the above constraints and resulted in approximately maximum probability of success.

#### 1.3.2 Design Characteristics

No major changes were made in the first stage Thor vehicle. The second stage, a welded type 410 stainless steel structure, is a basic AJ-10-40 tankage. The third stage consists of the ABL X-248-A3 rocket

motor and interconnecting structure. The payload shell, which is composed of a short cylindrical portion and two conical frustums, is made from honeycomb fiberglass. Equipment in the payload is mounted on the inner periphery of the cylindrical portion, which is locally reinforced where required. The nose cone fairing was designed to sustain aerodynamic loads and heating during first-stage operation.

The structure was designed to sustain design limit loads within the design environment without experiencing excessive yielding or deflections which would cause malfunction or failure of structure and components. Internal load distributions and critical loading conditions for each structural member were determined by analysis. The effects of extreme temperatures, transient heating, structural deflections, and dynamic loading were either included in the analyses, or conservative assumptions were made. Positive margins of safety were required and were shown analytically and/or demonstrated by test.

A number of loading conditions were considered in the structural design, including transportation and handling, prelaunch and flight. Dynamic considerations taken into account included bending modes and frequencies, axial and torsional modes and frequencies, and angular precession of the payload. Aerodynamic heating calculations were performed for various portions of the Able-1, and structural confirmation, and functional and dynamic tests were also made.

The first-stage Thor develops a sea level thrust of approximately 150,000 pounds and the engine is regeneratively cooled with RP-1. Thrust vector control is provided by gimbaling of the main engine. Two vernier engines each rated at 1000 pounds thrust are provided for roll control and final adjustment of burnout velocity.

The second stage, Aerojet Model AJ 10-101 rocket propulsion system, consists of a gimballed, regeneratively cooled thrust chamber, propellant tanks, helium pressurization system, interconnected plumbing, gimbal actuator, roll-control system, separation system for detachment from first stage and payload, necessary airframe structures and a destruct system.

The vehicle employed as the third stage of the Able-1 missile was a solid propellant motor which was developed by the Allegheny Ballistics Laboratory under contract with BuOrd. . This unit, developed as an advanced high-performance third stage for the Vanguard missile, had not been flight tested. Therefore, it was necessary for BMD/STL to evaluate the performance of this motor at altitude, prior to its use on Project Able-1.

The vernier and spin rockets utilized on the Able-1 Project were solid propellant units and were developed by the Atlantic Research Corporation for the Navy's Vanguard Program. Since these rockets were already qualified, confirmation of their altitude performance was the only remaining requirement prior to their use on the Able-1 vehicle. The confirmation was achieved through wind tunnel tests at AEDC at a simulated altitude of 100,000 feet.

The fourth stage or injection rocket for the Able-1 vehicle was a solid propellant motor developed by the Thiokol Chemical Corporation. The Thiokol TX8 motor was modified to include a new charge design and ignition system and was designated TX8-6. Development testing of this modified unit was conducted at Thiokol's Huntsville facility, and wind tunnel tests at a simulated altitude of 100,000 feet were subsequently performed at AEDC. This measured altitude performance confirmed the unit's capability of imparting the necessary velocity increment to the payload for establishing an orbit around the moon.

To increase the probability of lunar capture by decreasing the velocity dispersion existing at Stage III burnout, a total velocity increment of  $\pm 74$  ft/sec was available from eight small (50 lb-sec impulse) solid propellant vernier rockets mounted on a ring behind the payload. One to eight of these vernier rockets were to be fired on radio command from the ground to obtain the desired velocity increment. Determining the exact number of verniers which were needed and firing them was carried out at AFMTC.

The first-stage attitude control system was a standard Thor control system with modifications as required to accommodate the dynamics of the four-stage vehicle. These modifications consisted of relocating the rate gyros and redesigning the pitch and yaw frequency compensation networks.

The second-stage attitude control system was the same as the Project Able-0 system, and no design modifications were necessary. The major electrical components of the control system -- the gyros, amplifiers, demodulators, and associated hardware -- were basic Thor components.

The Able-1 Stage II electrical system consisted of a 400-cps inverter, a primary power battery, a relay junction box, an electrical cable system, and a destruct system filter.

The hangar testing of the Stage II electrical system consisted of the "covers-off" and "covers-on" tests. During these tests, the sequencing system was completely exercised and during "covers-on" test, the various igniter circuits were tested by actually detonating igniter squibs.

The missile power system was checked during "covers-on" tests by using an actual flight type battery and closely monitoring both the d-c power from the battery and the voltage and frequency of the inverter.

The equipment of the second-stage telemetry system included a transmitter, a voltage controlled oscillator, an electronic commutator, a pressure transducer, a power converter, and batteries.

The hangar checkouts in Florida are conducted using much of the same test equipment used later in the launch area. The Electrical Checkout Trailer is used in the hangar for the "covers-off" and "covers-on" tests. The trailer is equipped to simulate actual launch-complex conditions. Other pieces of equipment used for hangar checkout are later taken to the launch area for similar checkouts there. In this way, tests can be run under a close approximation of actual conditions.

Preparations and checkout on the launch stand included repetition of the system tests controlled from the blockhouse console, compatibility of the missile with the launch equipment and with the booster stage, and final sub-system calibrations. The following additional tests, which could be made in the hangar, were performed: signal strength measurements of the telemetry and of the payload package, r-f interference tests including the booster stage and payload, and command-destruct tests utilizing the first stage command-destruct equipment. Formal electrical system compatibility



and acceptance tests for both the Able stage and the booster stage are run soon after the missiles are mated. This test, together with a short propulsion leak test, suffices to qualify the Able stage for final calibration and sequence runs at T minus 2 and T minus 1 days.

The trajectory for the Able-1 mission required a high degree of precision in launching time. A period of approximately 20 minutes of each of four successive days constituted the permissible launch time for a given month. Experience with the basic Thor program and with the Thor-Able program showed that the use of a standard countdown would not result in this required timing accuracy. In consultation with Douglas Aircraft Operations Group in Florida, it was decided to incorporate several scheduled holds into the countdown. This resulted in a division of the countdown into the four major groups of tasks: second-stage propellant loading, electrical systems check, ordnance task, first-stage engine checks and fueling, tower removal, regulator setting and lox-ing, and terminal count.

### 1. 3. 3 Evaluation of Design

The operational reliability of each stage of the Thor-Able combination is believed to be satisfactory. The turbopump malfunction in the first stage of Missile 127 was corrected and the subsequent firings of Missiles 130 and 129 demonstrated satisfactory system operation. The performance of the first stage of Missile 130 was excellent and that of Missile 129 was well within normal limits.

The operation of the second stage was entirely satisfactory for both Missiles 130 and 129. Although there were indications of a low specific impulse in both flights, the total impulse available was more than adequate.

Analysis of the trajectory data from the flight of Missile 130 indicates that the total impulse of the third stage was probably within one-half per cent of its specified value. The failure of the third stage to ignite on Missile 129 is not attributed to an engine malfunction.

Vernier and spin rocket performance was as expected. No data are available on the fourth stage performance. However, it is believed that the failure of this stage to ignite during the flight of Missile 130 was caused

by a loss of battery power which resulted from the depressed temperature level on the altered trajectory.

All portions of the structure of the Able-1 appeared to perform properly. The structural loads encountered by Stages III and IV during the first stage operation were well below the design loads and hence indicate no structural failure or excessive deflections during this portion of the flight.

It is believed that all the structure was capable of carrying at least 1.25 times the maximum load that could be expected. No marginal areas of strength are known. The separation of the first and second stages and of the second and third stages depends upon the initiation of four explosive bolts in the first case, and upon two explosive bolts in the latter case. Reliability might have been improved if all bolts were not required to fire for satisfactory separation. The separation of Stages III and IV is accomplished by the firing of a single bolt and is quite reliable.

Missile 129 was modified in an attempt to overcome the approximate five degree trajectory deviation occurring during third stage firing of Missile 130. The most likely cause of this deviation was a thrust misalignment during the separation phase caused by a nozzle-blocking condition at the ignition created by the structural asymmetry of the compartment below the third stage nozzle. In addition, it was observed that the second stage spin rate decreased during the separation of the third stage from the second and may have contributed to the interference between the two stages. Four additional spin rockets, two retrorockets on the second stage, a trailing wire to the third stage igniter, and a pay-out basket for the excess wire were introduced on Missile 129. It was intended that the two stages should be separated by approximately one foot before firing the third stage.

The operation of the explosive bolts in the first/second stage separation was correct since satisfactory separation was attained in both the 129 and 130 flights. The separation bolts between the second and third stages of Missile 130 appear to have operated correctly in that the predictable maximum time lag between the two bolts could not have contributed sufficient impulse to cause the observed trajectory deviation. In the flight of Missile 129, it appears from an examination of the nutation frequency of

the separated stages that staging occurred, thus indicating that the second/third stage separation bolts operated correctly. Doppler data from Missile 130 and nutational frequencies from Missile 129 tabulated data both show that the third and fourth stages separated, thereby demonstrating proper bolt operation. The bolts and actuators which separate the nose shroud performed as expected during the flight of Missile 130. Preliminary analysis of the flight test data from Missile 129 indicates that the nose shroud separation mechanism operated correctly.

During Flight No. 1 the accelerometer appeared to function normally even though the telemetry signal indicated the improper magnitude. The unit uncaged at liftoff and completed 3.12 cycles of the output signal for an indicated velocity of 4368 ft/sec before termination of the flight at approximately 73 seconds. The performance of integrating accelerometer, Serial Number 14, on Flight No. 2 was satisfactory and no failures or indications of malfunctioning were detected.

The second stage inverter frequency again showed the characteristic trend which has appeared on all previous Able missiles, indicating that the average frequency over the flight period is approximately one-half cycle/second higher than the preflight frequency calibration.

The integrating accelerometer, Serial Number 15, for Flight No. 3 was modified to eliminate the cutoff command function and was connected as an arming circuit for doppler command cutoff. The accelerometer performance was normal in all respects and no indications of failures could be detected.

The second stage telemetry operation for all three flights was normal. Measurements were received, no dropouts have been noted. In all cases when the signal was lost, the cause was lack of line of sight.

In the three live operations that comprised the Able-1 program the vernier operation was completed satisfactorily. In each case the command was sent to fire all eight rockets.

## 1.4 Tracking and Communications

### 1.4.1 Ground Stations

Ground tracking stations were established by STL at AFMTC Florida, Hawaii, and Singapore, with the Jodrell Bank radio telescope installation of the University of Manchester in England also cooperating in the tracking operations. This telescope, together with an instrumentation trailer supplied by STL, provided a very powerful ground receiving facility. Another cooperating organization, the Millstone Hill, Mass., radar station of MIT also provided a tracking facility.

Calculations based on trajectory data received by teletype from the ground stations were performed at a central computing point at the STL Operations Center in Los Angeles to determine new estimates of the actual trajectory. The revised trajectory estimates were in turn used to calculate new steering data to assist the ground stations in the tracking operations.

The efforts of the primary ground system were assisted by many cooperating agencies. Arrangements were made with the NRL Control Center, Washington, D.C. for the relaying of tracking data from Minitrack stations to the Operations Center in Los Angeles via the STL communication center at Cape Canaveral. The Operations Center was also in contact with the NRL Center by telephone so that their interpretation of the Minitrack data would be readily available to the Operations Center. The presence of NRL technical personnel at the Operations Center during the October and November launches also greatly facilitated interpretation of the Minitrack data.

#### 1.4.1.1 Description of Ground Station Subsystems

Each ground station had a number of subsystems such as receivers, transmitters, data recording equipment, etc., which included among others, the following:

Phase-lock Receivers - All signals from the probe were received at 108.06 or 108.09 mc at each of the ground stations. Since these weak signals were to be detected in spite of noise, phase-lock receivers were used exclusively.

Command/Doppler Subsystem - The Able-1 lunar probe utilized a command/doppler system to fire vernier and retrorockets to improve the probability of lunar capture.

#### 1.4.1.2 Tracking Techniques

Several tracking techniques were used to determine the position of the satellite. These included the following:

- a. An AFMTC Azusa facility determined the trajectory of the first stage.
- b. The Millstone station skin-tracked the second stage using 400-mc long-range radar.
- c. Minitrack stations, operated by the Naval Research Laboratory, tracked the payload with two-axis interferometers.
- d. The command/doppler system at AFMTC measured radial range rate for the first sixteen minutes after launch.
- e. The Manchester station measured azimuth and elevation by tracking the telemeter transmitter at 108.06 mc from eleven minutes after lift-off for the full duration of the time for which the probe was above its horizon.
- f. The Millstone radar station switched to passive tracking with a phase-lock receiver about one-half hour after launch and gave azimuth and elevation data henceforth for all of the time the probe was above its horizon.
- g. The Hawaii station gave azimuth and elevation data from the 60-foot parabolic TLM-18 antenna for all the time the probe was above its horizon.
- h. The Hawaii station was equipped with a two-axis interferometer with a base line of 282 feet for each axis. It was hoped that this interferometer would give an angular accuracy of about 0.01 degree; however, the calibration of this subsystem proves difficult because of spurious reflections, with the result that no useful interferometer data was actually obtained.
- i. The Hawaii station was equipped with a command/doppler transmitter and doppler data extraction circuitry to permit the accurate measurement of two-way doppler.

j. The antenna system at the Singapore station had too broad a beam width to provide significant tracking information.

k. There was an attempt to track and photograph the probe with a large astronomical telescope at Palomar Observatory.

#### 1.4.1.3 Data Reduction and Storage

The following types of information were recorded and reduced for teletype transmission to the operations center in Los Angeles:

a. Telemetered information such as temperature, ionization, magnetic field, etc.

b. Direct observations of the carrier such as signal strength, polarization, signal strength fluctuations.

The data reduction process resulted only in quick-look information. Careful analysis of both Sanborn recordings and of the magnetic tape recordings in Los Angeles was also required to fully exploit the available information.

#### 1.4.1.4 Ground Station Communications and Data Transmission

The communication network of the Able-1 program was designed to fulfill two primary functions: (1) to provide orientation information rapidly to each of the ground tracking installations to enable them to locate and detect the beacon output of the fourth stage of the Able-1 vehicle, and (2) to process data rapidly as required for firing the fourth stage vernier rockets.

The location of stations and the general relationship of elements of the communication system are shown in Figures 1-26 and 1-27. The Operations Center functioned as the control point for the tracking network.

#### 1.4.1.5 Special Tracking and Photographing Task with an Astronomical Telescope

An attempt was made to obtain a photograph of a lunar probe for at least three reasons: (1) it would demonstrate the value and capabilities of optical instruments for measuring angular position, (2) several moderately-spaced optical observations would enable the fixing of a precise trajectory of the vehicle, and (3) a photograph of a missile on its way to the moon, or even far from earth, would have obvious prestige value.

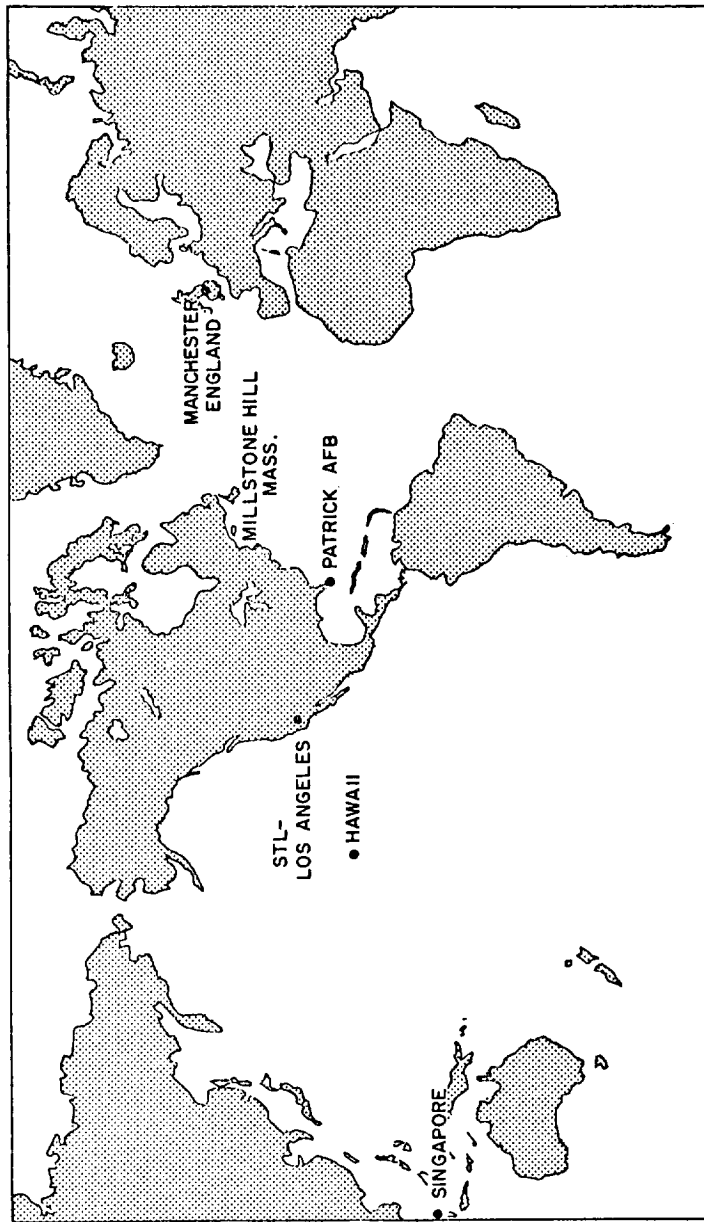


Figure 1-26. Ground Communication Net.





A detailed description of preparations undertaken for photographs of the lunar vehicle is contained in an Appendix (Volume III).

#### 1.4.1.6 Communications Office, AFMTC

The Able-1 vehicle was launched at AFMTC, where the launch data was gathered by the communications office. The launch and flight data necessary to support the Manchester station was sent from AFMTC communications office to the operations center in Los Angeles.

The communications office was in operation by 8 July 1958 for participation in prelaunch tests and support of the Able-1 program.

The Able ground station installation at AFMTC was intended as a launch control station and as a station for reception of telemetry signals after launch. This station was also responsible for checking of the payload and of the second stage doppler-command transceiver during countdown.

#### 1.4.1.7 Hawaii

Figure 1-28 is a photograph of the Hawaiian installation. There was very little man-made radio interference at this station.

The primary antenna at the Hawaii station was a 60-ft parabolic antenna mounted at the top of a 70-ft tower of steel and concrete. This antenna could be rotated through  $360^{\circ}$  in azimuth and through  $95^{\circ}$  in elevation. At its receiving frequency of 108.06 mc the antenna had a beamwidth of about  $8^{\circ}$ . The parabolic antenna was at the center of a group of four helical array antennas arranged in a square pattern with one diagonal north, south, east, west, forming an interferometer array. The distance across the diagonal was 262 feet. Each of the helical array antennas consisted of four helices.

The Hawaii station had a complete dual receiving installation consisting of a pair of phase-lock receivers which could receive 108.06- or 108.09-mc signals, two Ampex tape recorders, two Sanborn galvanometer recorders, and a double set of voltage-controlled oscillators. This dual installation allows simultaneous recording of telemetry from two frequencies.



Figure 1-28. The Hawaii Ground Station.

The communication equipment at Hawaii was teletypewriter-perforator set with service maintained eight hours per day and increased to 24 hours during operations.

#### 1.4.1.8 Manchester

The Manchester station was located near Manchester, England, at the Jodrell Bank radio telescope installation of Manchester University. This radio telescope, a photograph of which is shown in Figure 1-29 had a 250-foot antenna as its primary facility.

Operation at Manchester was a cooperative venture in which the British supplied personnel to operate their antenna steering system and STL supplied personnel to operate the receivers and instrumentation portion of the system.

The 250-foot antenna had a bandwidth of  $2^{\circ}$  at the frequency of 108 mc used for the Able-1 program. The antenna feed (constructed by the British) performed very well.

The antenna system tracked the space probe by carefully plotting signal strength as the elevation angle (or as azimuth angle) changed by discrete steps. Plots obtained in this way were symmetrical and allow determination of the actual elevation (or azimuth angle) to better than  $1/4^{\circ}$  accuracy.

The Space Technology Laboratories trailer included a single microlock receiver which could be tuned to 108.06 mc or 108.09 mc at the operator's choice.

An Ampex FR-107 tape recorder was used to record both the phase modulation and the amplitude modulation signals from the microlock receiver. Timing signals, voice commentary and a group of voltage-controlled oscillators for the recording of gain control bias, signal strength, etc., were also recorded.

The phase-lock receiver output (which contained the telemetered information from the payload) was recorded on magnetic tape and also in a Sanborn recorder after being demodulated by a bank of Hallamore subcarrier discriminators.

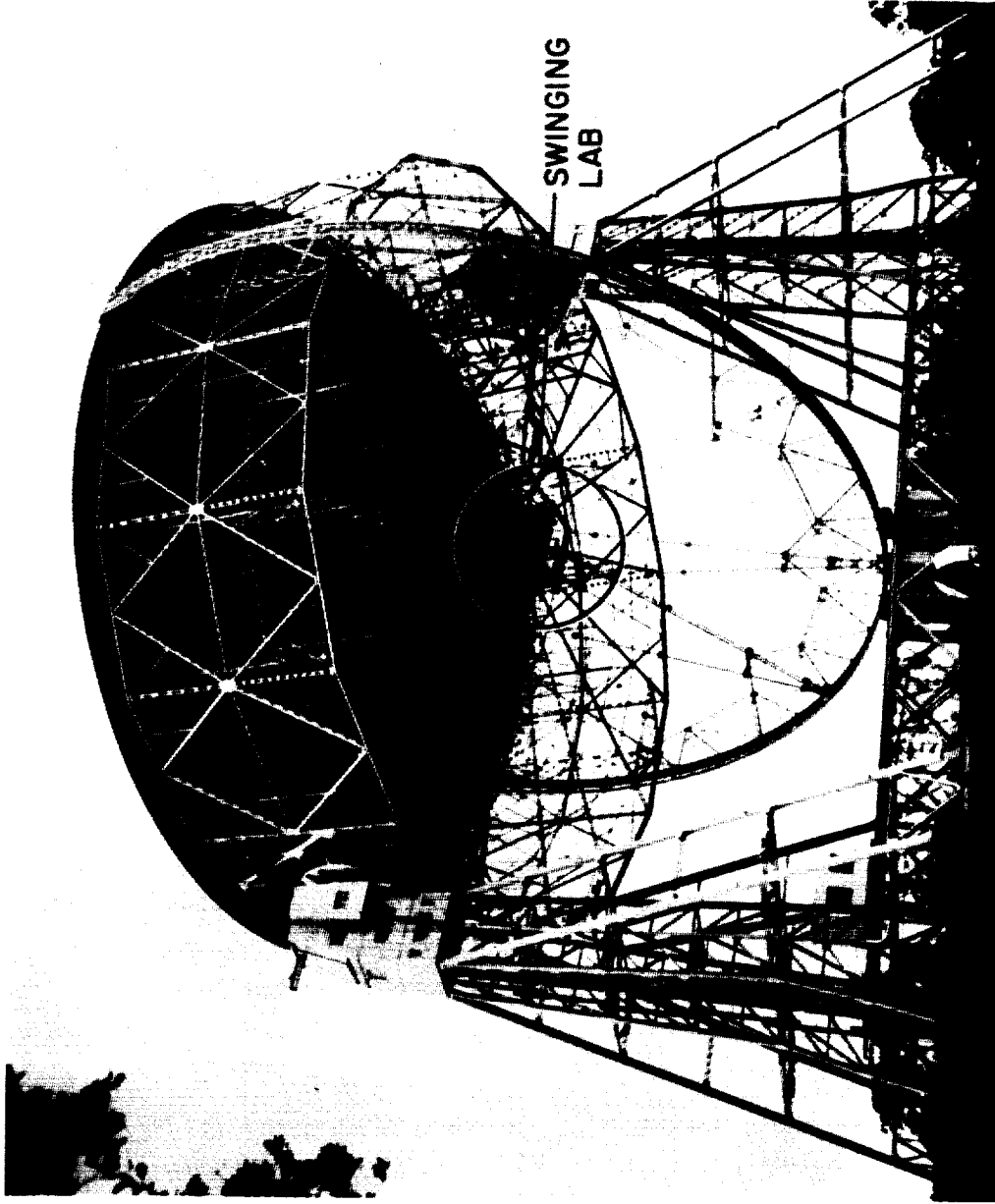


Figure 1-29. Manchester Tracking Station Showing STL Facility.

#### 1.4.1.9 Singapore

The Singapore station was located about 5 miles north of this city on the receiving antenna farm of Cable and Wireless, Ltd. One helical array antenna, instrumentation trailer, and deisel-driven generators were located in a vacant field near a row of bungalows which are used normally for housing of Cable and Wireless personnel. One of these bungalows was made available to STL for use as an office and ready room.

The single helical array antenna was physically identical to each of the array antennas of the interferometer at the Hawaii station. This antenna had about 19 db of gain over an isotropic radiator and a bandwidth of about 30°. One-speed electric motor allows the antenna to be pointed in any direction.

The instrumentation was very similar to that provided at Manchester. This included a phase-lock receiver, an Ampex tape recorder, a Sanborn chart recorder, and two distriminators to demodulate the telemetered information from the lunar probe for display on the Sanborn recorder.

Communication from Singapore to the Operations Center at STL was established by radio teletype.

#### 1.4.1.10 Millstone

The MIT Lincoln Laboratories operated a large tracking radar facility at Millstone Hill, Mass. It is an 84-foot parabolic reflector and has a gain of approximately 26.8 db at 108 mc/sec.

Communications between Millstone and the STL Operations Center were accomplished by teletype TWX service. During tracking operations teletype service was continuous. Long distance telephone service was also used between Millstone and AFMTC.

#### 1.4.1.11 Malabar Station, Melbourne, Florida

At Melbourne and Florida, RCA and Radiation Incorporated jointly operate a 60-foot diameter reflector manufactured by D. S. Kennedy and Company. This dish is quite similar to the one at South Point, Hawaii, and was used for telemetry.

#### 1.4.1.12 Army Ballistic Missile Agency

The Army Ballistic Missile Agency at Cape Canaveral and Huntsville, Alabama used a six-turn helix and a 60-foot diameter Kennedy reflector respectively as tracking antennas on 108.09 mc.

#### 1.4.2 Functioning of Ground Stations During Flights

##### 1.4.2.1 AFMTC Station

During each launch, the AFMTC station participated heavily in count-down activities to ensure proper functioning of the airborne counterparts to the doppler/command telemetry ground equipment.

##### 1.4.2.2 Millstone Station

Millstone station successfully acquired the second stage on their 400-mc radar during the October and November shot, and skin-tracked the second stage for some minutes after separation of the second and third stages.

##### 1.4.2.3 Manchester Station

The Manchester station acquired the payload on both the October and November flights and tracked it as long as it was above the local horizon. For the October flight this tracking period lasted for several hours on each of two days; for the November flight, the payload was very low on the horizon and was tracked only sporadically and for a few minutes as it passed to the south of the station.

During the October flight the flight path deviated from the predicted path by approximately 13 degrees; this deviation caused the initial acquisition (made about 11 minutes after launch) to be made on a minor lobe of the antenna. After about 40 minutes of tracking (with a signal that appeared to be very weak) the error was corrected and further tracking was done with the main lobe. Accuracy of tracking data from Manchester was excellent, and the telemetry data was very good due to the large aperture of the antenna at that station.

##### 1.4.2.4 Hawaii Station

The Hawaii station participated only in the October flight, since the other two flights did not traverse that part of the world. During the October flight the payload was tracked from the time it rose above the horizon until it

sank below the horizon at the end of the tracking day. On the second day the payload was tracked as it approached the earth and was finally lost as it plunged toward the earth in the southeastern Pacific region.

Tracking and telemetry data were obtained throughout. Tracking data was better than expected from the 60-foot dish.

The doppler-command system was used a number of times on both tracking days in attempts to fire the retrorockets and to release the vernier rocket ring. Indications were frequently received that the payload had detected and momentarily acquired the ground transmitter carrier; however, the cold batteries in the payload were evidently not sufficiently powerful to fire the squibs and thus execute the commands.

#### 1.4.2.5 Singapore Station

The Singapore station participated only in the October flight, since the other two flights did not traverse that part of the world. During the October flight the payload was tracked from the time it rose above the horizon until it sank below the horizon at the end of the tracking day.

#### 1.4.3 Data Handling: Able-1 Operations Center

The BMD/STL Operations Center was established in Los Angeles to control and coordinate all data handling and decision processes that were to occur during the flight. The specific purposes of the Operations Center were the processing of tracking data received from the ground tracking stations, the determination of the actual trajectory from the tracking data, the derivation and transmission of revised steering data for ground station antenna, interpretation of quick-look telemetry data received from the ground stations during flight, and the making of decisions as to the time of command transmission for dropping the vernier cluster and firing the retrorocket. Nominal trajectory data were derived before the flight and transmitted to the Able-1 ground stations as well as to certain other cooperating stations. These data were used to plan nominal steering periods and to control antenna steering until more accurate data based on actual tracking were received from the Operations Center.

#### 1.4.4 Trajectory Determination for Specific Flights

##### 1.4.4.1 August Flight - Missile 127

The Operations Center was manned at approximately T minus 6 hours. Earlier informal checks of station readiness were confirmed by teletype. Discussions between Los Angeles and Cape Canaveral indicated the desirability of an early formal statement of ground station readiness by the Operations Center. Plans for later flights were changed to incorporate the T minus 6 hour readiness report. The planned computer checkout was performed. At the time of lift-off, the Operations Center was in contact with Manchester, Millstone, and AFMTC, and the Operations Center and all participating ground stations were in a state of readiness.

##### 1.4.4.2 October Flight - Missile 130

Preliminary readiness checks were made with all STL ground stations during the day of 10 October 1958. A preliminary readiness report was made to AFMTC, stating that all ground stations were ready. The Operations Center was fully manned at T minus 4 hours. At the time of lift-off, all ground stations and the Operations Center were in a state of readiness.

The best estimates available of the trajectory based upon all available data are as follows:

Launch time	0342/13 EST 11 October 1958
Burnout conditions time	0347/20 EST
altitude	1,410,000 feet
latitude	30.70° N
longitude	71.07° W
velocity magnitude	34,524.5 ft/sec
velocity azimuth	70.43°
velocity angle	
from vertical	64.74°
Maximum altitude (from surface)	70,717 statute miles (61,452 nautical miles)
Re-entry time after lift-off	43 hours 17.5 minutes
latitude	21.0° S
longitude	88.1° W



Figure 1-30 compares the actual tracking data of the Manchester Station with the theoretical tracking data calculated on the basis of the final trajectory parameters summarized above. Figure 1-31 shows the projection on the earth of the vehicle path in the plane of the moon's orbit.

#### 1.4.4.3 November Flight - Missile 129

Preliminary readiness checks were made during the day of 6 November 1958. All ground stations were ready with no serious trouble except for the amplifier in the transmitter at the Hawaii station, and since this trouble was in the process of being corrected by T minus 6 hours, a preliminary readiness report was made to AFMTC, stating that all ground stations would be ready. The Operations Center was fully manned at T minus 4 hours. When the decision to delay the launching one day was made, all ground stations were informed that, pending further clarification, a full countdown including ground station readiness checks would begin the following morning. During 7 November, the regular preliminary readiness checks were made and a report was made to AFMTC at approximately T minus 6 hours that all ground stations were ready. The Operations Center was again fully manned at T minus 4 hours. At the time of lift-off, all ground stations and the Operations Center were in a state of readiness. The Operations Center received from AFMTC by teletype the lift-off time. Shortly after second stage burnout, AFMTC reported by telephone to the Operations Center that the doppler data indicated that the third stage had not ignited. While a computer run based upon second stage nominal burnout conditions was being run, graphical estimates of the trajectory were derived in an attempt to aid Manchester in acquiring the vehicle. Tracking data of varying degrees of reliability were received from Manchester, Slough, Fort Monmouth, Malabar, Millstone, and AFMTC. The general conclusion has been reached that the most accurate estimate of burnout conditions is that obtained from the data derived from powered flight tracking at Cape Canaveral aided by Millstone skin-tracking data. The limited amount of free flight tracking data obtained compares favorably enough with the trajectory obtained from the powered flight estimate to serve as a general confirmation but do not seem to be sufficiently consistent to permit the derivation of a more accurate burnout estimate. The parameters associated with the best estimate of the trajectory are:

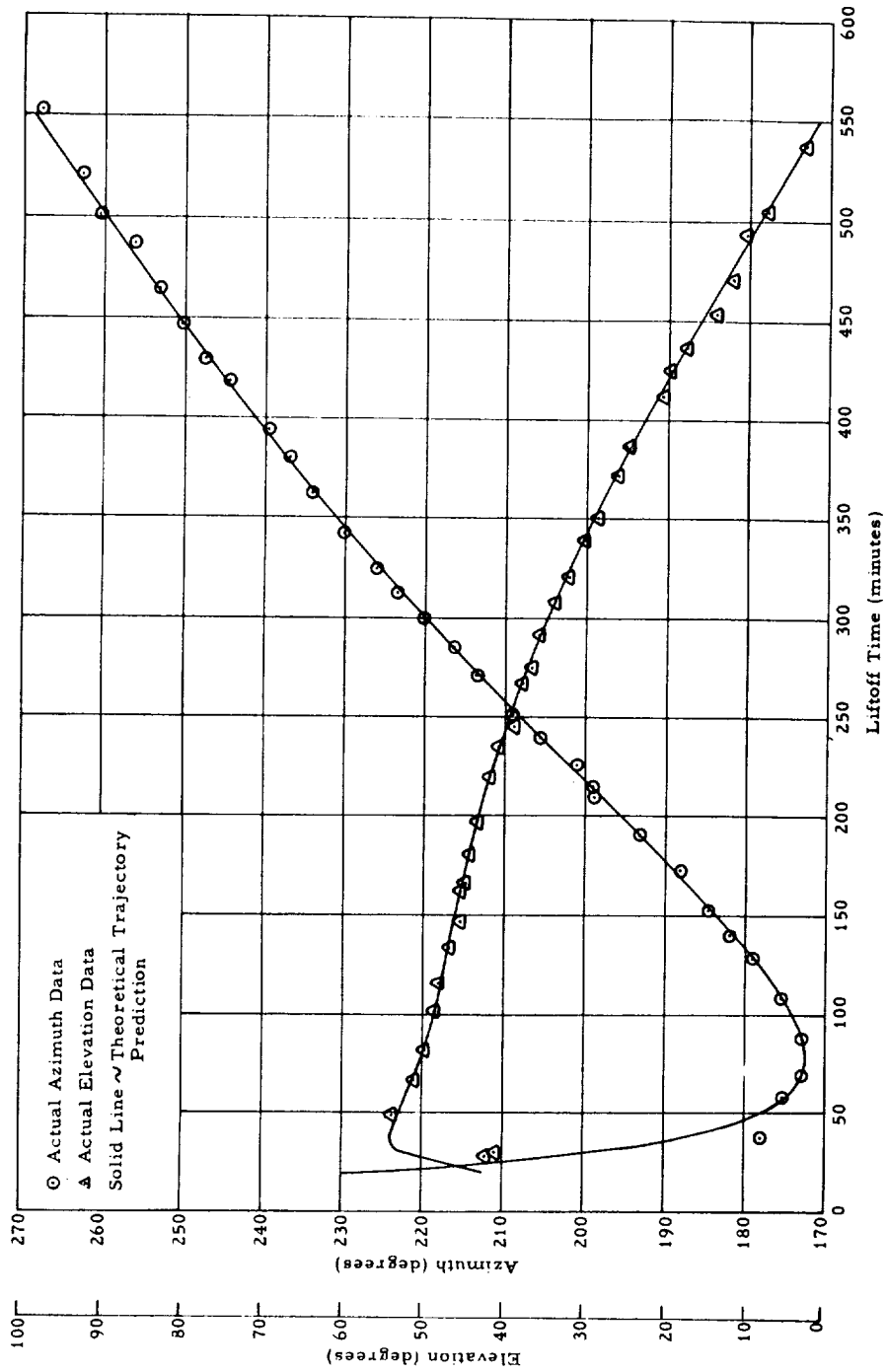


Figure 1-30. Actual Tracking Data of Manchester Compared with Theoretical Tracking.

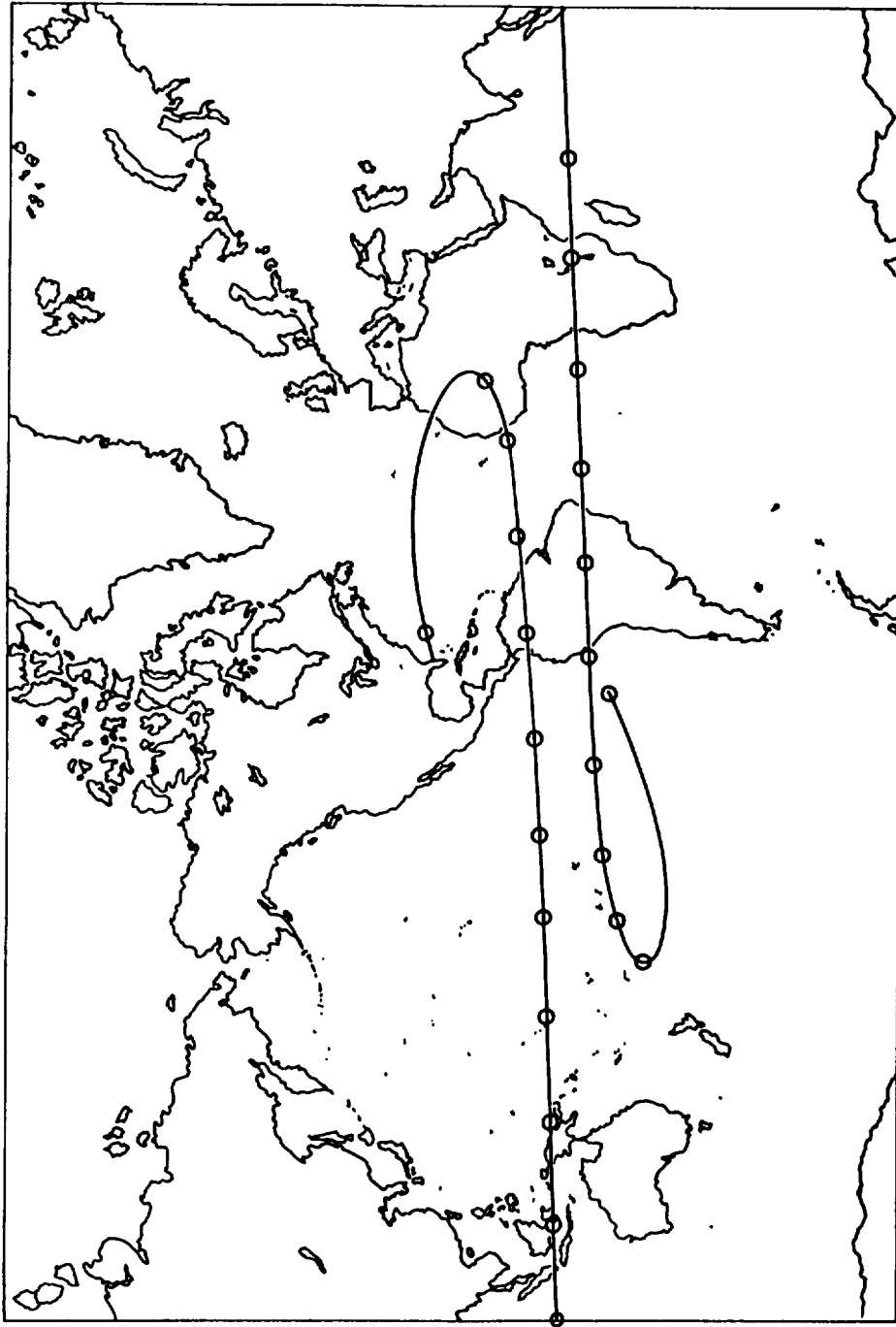


Figure 1-31. Projection on Earth of Path of Flight 2. First point is burnout; subsequent points are at two-hour intervals after burnout.

Launch time	0230/21 EST 8 November 1958
Burnout conditions time	
altitude	1,003,000 feet
latitude	29.63°N
longitude	73.7°W
velocity	
magnitude	23,616 ft/sec
velocity azimuth	77.0°
velocity angle from vertical	71.5°
Maximum altitude (from surface)	963 statute miles (836 nautical miles)
Re-entry time after lift-off	37.85 minutes
latitude	28.7°N
longitude	1.85°E

Figure 1-32 shows the Pioneer II trajectory projection on the surface of the earth.

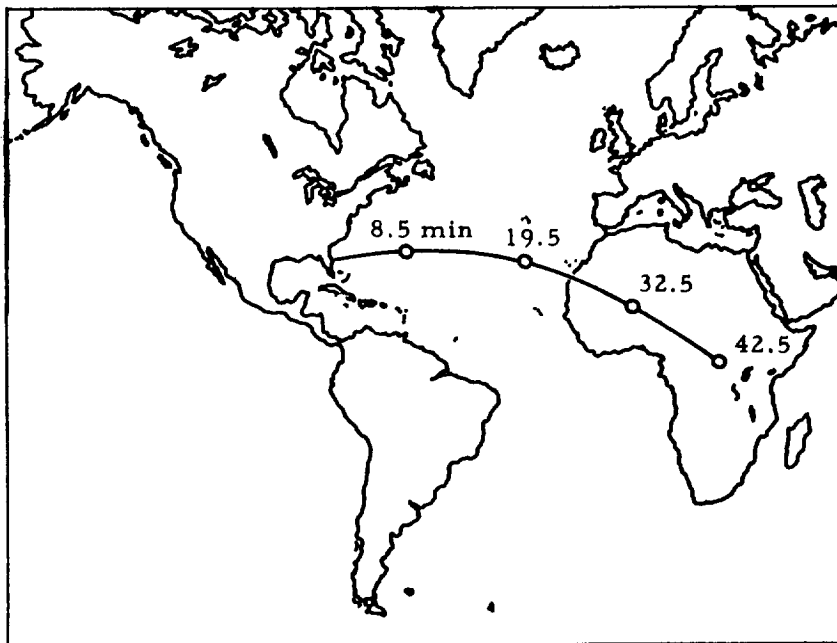


Figure 1-32. Pioneer II, Projection of the Path of Flight 3 on the Earth's Surface.

## 1.5 Flight Summaries

The launchings of the three Able-1 vehicles were for the most part uneventful and proceeded as scheduled with the exception of a one-day delay in the launch of Flight 3. Flight 1 (No. 127) was launched on 17 August 1958, Flight 2 (No. 130) on 11 October 1958, and Flight 3 (No. 129) on 7 November 1958.

### 1.5.1 First Lunar Probe

The first lunar probe was installed on Thor Missile Number 127. The missile was launched at 0718 EST on 17 August 1958, which was only 4 minutes later than the scheduled launch time of 0714 EST. The flight was normal until 73.6 seconds after lift-off when a turbopump bearing failed and the lox pump stopped.

Analysis of the flight test telemetry indicated proper control system operation and showed that the missile was about 0.2 degree high at the time of the explosion. This value was much less than on some of the Project Able flights for a corresponding flight time, thereby indicating that the inclusion of a programmer had indeed contributed significantly to the velocity vector dispersions noted on the previous missiles.

### 1.5.2 Second Lunar Probe

For the second probe, the booster was Thor Missile Number 130. The missile was launched at 0342 EST on 10 October 1958, only 13 seconds later than the scheduled time. Excellent performance was obtained from both the first and second stages. At first-stage engine shutdown the velocity was about 800 ft/sec greater than nominal, and the velocity vector was about 2.5 degrees high.

A smooth transition to second stage operation was accomplished, and a second stage burning time of 104 seconds was obtained. Engine shutdown was commanded by the integrating accelerometer, and the velocity at this time was between 23,125 and 23,150 ft/sec or about 190 ft/sec less than the desired velocity. This difference was primarily due to the fact that the integrating accelerometer computed along a lofted trajectory. At shutdown, the velocity vector was lofted by 3 degrees.

At third stage burnout, the inertial velocity was approximately 500 ft/sec less than the desired value of 35,206 ft/sec. Subsequently, all vernier rockets were fired in an attempt to make up the velocity deficit, but their impulse was not sufficient, and escape velocity was not achieved. The fourth stage reached an altitude of 71,700 statute miles, and good payload telemetry data were obtained during the flight.

An attempt was made to convert the payload into a high altitude satellite by firing the fourth stage, but, because of low internal temperatures, the missile batteries were incapable of supplying the ignition current.

Free flight tracking data indicated that the velocity vector was about 5 degrees off in azimuth at third stage burnout which implies that the third stage must have been disoriented approximately 16.2 degrees in the yaw axis and pitched up 14.8 degrees. Considerable effort was expended in the analysis of possible causes contributing to such a disturbance. Several causes which were considered and discarded were: (1) failure of one or more of the eight spin rockets, (2) gyro drift during second stage, (3) third stage thrust misalignment, (4) second stage thrust tail-off, and (5) bucking or failure of structure coupling the second and third stages. Consideration of the momentum properties of the missile indicated that an impulse of only 11 lb-ft/sec could change the momentum vector of the third stage by 15 degrees. Since the third stage is ignited while it is still in contact with the second stage, and since the third stage nozzle rests on a beam that is not symmetrically located with respect to the nozzle, such a disturbance could have been caused by asymmetrical gas flow during the separation. Accordingly, provisions were made to prevent such action in the third missile. Retrorockets were installed on the second stage, and the third stage fire signal was delayed one second after retrorocket firing.

The hypothesis of a large angular disturbance at the initiation of Stage III is consistent with both the measured range rate and free flight data and a theoretical description of the dynamics of a rocket given such an initial disturbance. It is also indicated that the performance of the ABL 248 rocket was within one-half per cent of the predicted value.

### 1.5.3 Third Lunar Probe

The booster for the third lunar probe was Thor Missile Number 129. Launch was at 0230 EST, 8 November 1958, 31 seconds after the scheduled launch time for that day. The first stage control system performed satisfactorily, and the cutoff velocity was 200 ft/sec greater than, 1.5 degrees lower than, and 2.3 degrees to the left of nominal.

Second stage operation was completely normal, and the velocity at shutdown was within 40 ft/sec of the desired value. Engine shutdown was commanded by a signal from the ground to a doppler command system which had been installed in the missile payload to reduce the velocity error incurred on the second flight. The spin rockets were ignited and the proper spin velocity of 2.1 rps was achieved. The third stage was separated, but it failed to ignite and the vehicle failed to escape. There is no clear-cut explanation for the failure of the third stage. It may be attributed to several causes: (1) a break in the wire to the igniter, (2) failure of the igniter, (3) a poor connection to the igniter, or (4) a failure in the firing signal transmitter.

All tracking stations operated satisfactorily. The payload was tracked for approximately 15 minutes by the tracking facility at Cape Canaveral, but, because of the failure of the third stage, the signals were not obtained at the Manchester station.

The performance of the first stage propulsion system was high but within nominal limits for all flights with the exception of Missile 127. Sufficient impulse was available to provide the required velocity at second stage burnout. Satisfactory electrical and electronic mechanical functioning was demonstrated during the second stage.

It is believed that the third stage of Missile 129 did not receive the firing command from the third stage. This has been attributed to the breaking during second/third stage separation.

An attempt was made to fire the vernier rockets after payload separation. Doppler range rate indicated no velocity change, which implies that either the verniers did not fire or that they fired at an angle very greatly different from nominal.





